

# Earth and Space Science



## RESEARCH ARTICLE

10.1029/2022EA002532

### Key Points:

- The Mars 2020 Mastcam-Z investigation's stereoscopic zoom camera pair enables the assembly of 3D models of the rover environment
- Processing and visualization for scientific 3D data exploitation establishes mission science in full knowledge about spatial relationships
- Important scientific use cases for Mastcam-Z 3D vision processing and visualization illustrate the importance of 3D for Mars science

### Supporting Information:

Supporting Information may be found in the online version of this article.

### Correspondence to:

R. Barnes,  
[robert.barnes@imperial.ac.uk](mailto:robert.barnes@imperial.ac.uk)

### Citation:

Paar, G., Ortner, T., Tate, C., Deen, R. G., Abercrombie, P., Vona, M., et al. (2023). Three-dimensional data preparation and immersive mission-spanning visualization and analysis of Mars 2020 Mastcam-Z stereo image sequences. *Earth and Space Science*, 10, e2022EA002532. <https://doi.org/10.1029/2022EA002532>

Received 25 JUL 2022

Accepted 3 FEB 2023

### Author Contributions:














**Conceptualization:** Gerhard Paar, Andreas Bechtold

**Data curation:** Gerhard Paar, Christian Tate, Robert G. Deen, Parker Abercrombie, Andreas Bechtold, Fred Calef, Robert Barnes, Ken Herkenhoff

**Formal analysis:** Robert Barnes, Christian Koeberl, Christoph Traxler, Sanjeev Gupta

**Funding acquisition:** Gerhard Paar

## Three-Dimensional Data Preparation and Immersive Mission-Spanning Visualization and Analysis of Mars 2020 Mastcam-Z Stereo Image Sequences

Gerhard Paar<sup>1</sup> , Thomas Ortner<sup>2</sup> , Christian Tate<sup>3</sup>, Robert G. Deen<sup>4</sup> , Parker Abercrombie<sup>4</sup>, Marsette Vona<sup>4</sup>, Jon Proton<sup>5</sup> , Andreas Bechtold<sup>6,7</sup> , Fred Calef<sup>4</sup> , Robert Barnes<sup>8</sup> , Christian Koeberl<sup>6,7</sup> , Ken Herkenhoff<sup>9</sup> , Elisabeth M. Hausrath<sup>10</sup> , Christoph Traxler<sup>2</sup> , Piluca Caballo<sup>1</sup>, Andrew M. Annex<sup>11,12</sup> , Sanjeev Gupta<sup>8</sup>, James F. Bell III<sup>13</sup>, and Justin Maki<sup>4</sup> 

<sup>1</sup>JOANNEUM RESEARCH Forschungsgesellschaft mbH, Institute for Information and Communication Technology, Graz, Austria, <sup>2</sup>VRVis Zentrum für Virtual Reality und Visualisierung Forschungs-GmbH, Vienna, Austria, <sup>3</sup>Department of Astronomy, Cornell University, Ithaca, NY, USA, <sup>4</sup>NASA Jet Propulsion Laboratory (JPL), California Institute of Technology, Pasadena, CA, USA, <sup>5</sup>Opscode LLC, San Diego, CA, USA, <sup>6</sup>Austrian Academy of Sciences, Vienna, Austria, <sup>7</sup>University of Vienna, Department of Lithospheric Research, Vienna, Austria, <sup>8</sup>Department of Earth Science & Engineering, Imperial College, London, UK, <sup>9</sup>U. S. Geological Survey Astrogeology Science Center, Flagstaff, AZ, USA, <sup>10</sup>Department of Geoscience, University of Nevada, Las Vegas, NV, USA, <sup>11</sup>Division of Geological and Planetary Sciences, California Institute of Technology, Pasadena, CA, USA, <sup>12</sup>Morton K. Blaustein Department of Earth & Planetary Sciences, Johns Hopkins University, Baltimore, MD, USA, <sup>13</sup>School of Earth and Space Exploration, Arizona State University, Tempe, AZ, USA

**Abstract** The Mars 2020 Mastcam-Z stereo camera investigation enables the generation of three dimension (3D) data products needed to visualize and analyze rocks, outcrops, and other geological and aeolian features. The Planetary Robotics Vision Processing framework “PRoViP” as well as the Instrument Data System on a tactical—sol-by-sol—timeframe generate 3D vision products, such as panoramas, distance maps, and textured meshes. Structure-from-motion used by the Advanced Science Targeting Toolkit for Robotic Operations (ASTTRO) “Landform” tool and long baseline stereo pipelines add to the 3D vision products' suite on various scales. Data fusion with textured meshes from satellite imagery and 3D data analysis and interpretation of the resulting large 3D data sets is realized by visualization assets like the Planetary Robotics Vision 3D Viewer PRo3D, the 3D Geographical Information System GIS CAMP (Campaign Analysis Mapping and Planning tool), the ASTTRO 3D data presentation and targeting tool, and the Mastcam-Z planning tool Viewpoint. The pipelines' workflows and the user-oriented features of the visualization assets, shared across the Mars 2020 mission, are reported. The individual role and interplay, complements and synergies of the individual frameworks are explained. Emphasis is laid on publicly available 3D vision data products and tools. A representative set of scientific use cases from planetary geology, aeolian activity, soil analysis and impact science illustrates the scientific workflow, and public data deployment modes are briefly outlined, demonstrating that 3D vision processing and visualization is an essential mission-wide asset to solve important planetary science questions such as prevailing wind direction, soil composition, or geologic origin.

**Plain Language Summary** Image processing enables to describe the surface of Mars in three dimension (3D) using the Mastcam-Z stereo cameras' images. The 3D reconstruction of the rocks, geological outcrops, as well as aeolian and mineralogical features, are crucial for understanding the planet's past. Image processing tools to reconstruct the surface of Mars from the images are available to the Mars 2020 Team, generating 3D data products with various information about the surface on Mars like elevation maps or distance maps that record the 3D coordinates of each point. To interpret these products, tools needed for their visualization and analysis are presented here. In a combination with data from other sensors or sources—including 3D models obtained from satellite, and at different scales the interpretation of the processed products is enhanced. The reader learns about the synergies and interplay between these tools, including publicly available tools. Demonstrative planetary science examples, processed by the Mastcam-Z science team with the above mentioned tools, are presented. Geological features, such as wind activity, soil analysis, and impact science, are analyzed, illustrating the scientific work carried out and in particular the benefit of 3D vision processing and visualization for such analysis work.

© 2023 The Authors. Earth and Space Science published by Wiley Periodicals LLC on behalf of American Geophysical Union.

This is an open access article under the terms of the [Creative Commons Attribution License](https://creativecommons.org/licenses/by/4.0/), which permits use, distribution and reproduction in any medium, provided the original work is properly cited.

**Investigation:** Andreas Bechtold, Fred Calef, Robert Barnes, Ken Herkenhoff, Elisabeth M. Hausrath, Andrew M. Annex  
**Methodology:** Gerhard Paar, Christian Tate, Robert G. Deen, Parker Abercrombie, Jon Proton, Andreas Bechtold, Fred Calef, Robert Barnes, Ken Herkenhoff, Elisabeth M. Hausrath, Christoph Traxler, Andrew M. Annex, Sanjeev Gupta  
**Project Administration:** Gerhard Paar  
**Resources:** Gerhard Paar  
**Software:** Gerhard Paar, Thomas Ortner, Christian Tate, Robert G. Deen, Parker Abercrombie, Marsette Vona, Jon Proton  
**Supervision:** Gerhard Paar, Christian Koeberl, Christoph Traxler, Sanjeev Gupta, James F. Bell III  
**Validation:** Andreas Bechtold, Robert Barnes, Andrew M. Annex  
**Visualization:** Gerhard Paar, Thomas Ortner, Christian Tate, Parker Abercrombie, Marsette Vona, Jon Proton, Andreas Bechtold, Fred Calef, Robert Barnes, Christoph Traxler  
**Writing – original draft:** Gerhard Paar, Thomas Ortner, Christian Tate, Robert G. Deen, Parker Abercrombie, Marsette Vona, Jon Proton, Andreas Bechtold, Fred Calef, Robert Barnes, Ken Herkenhoff, Elisabeth M. Hausrath, Christoph Traxler, Andrew M. Annex  
**Writing – review & editing:** Gerhard Paar, Christian Koeberl, Christoph Traxler, Piluca Caballo, Sanjeev Gupta, James F. Bell III, Justin Maki

## 1. Introduction

### 1.1. Mission and Instrument Context

The NASA Mars 2020 Perseverance Rover mission landed in Jezero Crater on Mars on 18 February 2021, to undertake the next key steps in our understanding of Mars' potential as a habitat for past or present life. By 14 June 2022, Perseverance has traveled 12,052.7 m and has collected eight rock core samples and one atmospheric sample.

Among other science instruments (Maki et al., 2020; NASA, 2021), Perseverance carries Mastcam-Z, a twin zoomable multispectral camera. The stereo camera configuration of Mastcam-Z offers 3D vision capabilities to gain 3D reconstructions of the outcrops and geological features encountered by Perseverance, which is used, for example, for distance/height and orientation measurements for topographic and structural analysis of the rover's surrounding in true scale (Bell et al., 2021). The instrument underwent a thorough calibration process to assign its geometric and radiometric capabilities to physically true observations (Hayes et al., 2021).

### 1.2. Scope and Objectives

This paper provides an overview of the 3D vision and visualization components that are available and in tactical (=used for daily planning) and strategic (longer-term planning and scientific exploitation) use of the Mastcam-Z stereoscopic data. It intends to raise understanding on the 3D vision and visualization methods used within the Mars 2020 Science team, with emphasis on the Mastcam-Z Instrument, to learn about the data curation and analysis methods for spatial understanding and interpretation of the data, to understand how science findings are supported by knowledge about spatial relationships and quantitative information about dimensions and morphology. The description of methods and their interplay is underlined by relevant science use cases.

It is not the primary aim of this paper to provide a basis to allow to re-create all the work being done using all the tools presented here. It shall on the one hand raise understanding of the existing data products and their interpretation to be able to assess their integrity, and on the other hand get inspired how the 3D data processing and visualization could be improved, complemented, and expanded. It shall also explain the rationales and implications of imaging constraints (and ultimately the limits) that are posed by the 3D vision processing and data presentation methods. It is meant to complement earlier and contemporary publications that expand on the Mastcam-Z instrument and objectives itself (Bell et al., 2021), and its calibration (Hayes et al., 2021), and act as a reference for the use-case driven methods used in future publications.

The Mastcam-Z mission operations and data exploitation involves numerous international teams working on the science exploitation and provision of the engineering assets and data. Those teams have primary access to the downlinked data, and a specific infrastructure is set-up on NASA JPL premises in mission context for the data processing (Instrument Data System [IDS], Landform, see Sections 4.2 and 4.3) and visualization (Campaign Analysis Mapping and Planning [CAMP], Advanced Science Targeting Toolkit for Robotic Operations [ASTTRO], see Sections 5.2 and 5.3), with the instruments' Principal Investigator (PI) Teams in addition setting up their own portals for the respective instrument teams to make available calibrated products and enable uplink planning (Viewpoint, Section 5.4). Those tools, except the MMGIS core of CAMP, are intended to be used by the mission team only.

Whilst daily browse products are made available to the public in raw or sparsely processed form, quarterly PDS releases enable the access to the calibrated mission data sets (Section 7). Apart from those standard access cases known from prior Mars exploration missions, the Mastcam-Z Team offers public access to 3D vision products and visualization being heritage of ExoMars PanCam development (Coates et al., 2017), or Structure-from-Motion by commercially or open-access available tools, these assets (PRoViP and PRo3D and Structure-from-Motion approaches) are covered in Sections 4.1, 5.1, and 4.4, respectively.

## 2. Overview on Mastcam-Z Processing and Visualization

To operate a camera instrument on the surface of Mars and exploit its data, various techniques and tools are employed. In summary, the following steps apply in the context of Mastcam-Z science data exploitation.

1. Planning assesses the current environment and scientific needs and assembles a set of commands that are uplinked to the Rover on-board software to be executed in due time.

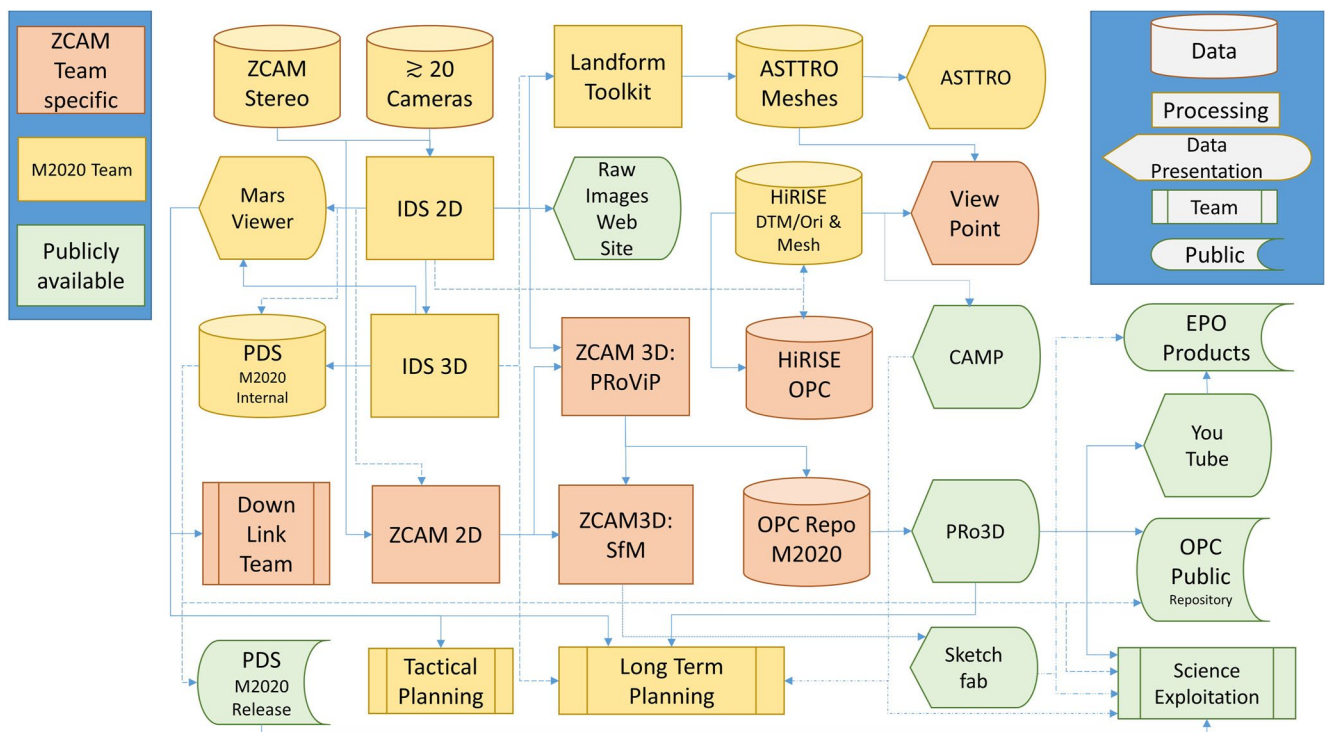


**Figure 1.** Mastcam-Z—relevant data entities, processing frameworks and visualization/data presentation tools, and their accessibility (simplified). ZCAM, Mastcam-Z; M2020, Mars 2020; PDS, Planetary Data System; EPO, Education, Publication and Outreach; SfM, Structure-from-Motion.

2. For command execution on-board the rover, the operations team takes into account various rules and conditions (mainly in terms of timing and sequencing) to launch a cadence of imaging commands—typically about 100 images per Sol (see Text S1 in Supporting Information S1 for a downlink amount example).
3. The gained data sets are compressed, downlinked to Earth and distributed to the tactical teams via a central data repository. Meta data accompanying the images make sure that the context of imaging is properly documented and taken into account during further processing.
4. Processing is launched at various levels, from fully automatic preprocessing to obtain automatically calibrated data products, to sophisticated manually operated software tools. At tactical time frame such processing takes place within a few minutes to hours, further data exploitation takes place in strategic time frame within days or for further scientific use over months and years.
5. Tactical and in part also strategic processing results are further used to drive the decisions of the next planning cycle—in most cases as an interplay of data coming from various instruments.

Most of these steps are taken inside the mission context, infrastructure, and teams. Figure 1 illustrates the interplay of input/output/intermediate data, processing and visualization tools and their accessibility, as well as specific “customers” of the given entities. The following main components are involved.

1. Mastcam-Z stereo images (Section 3.1) are the primary source for scientific close-range Mars 2020 vision data products. Besides Mastcam-Z, Perseverance carries a comprehensive suite of imaging instruments (NASA, 2021).
2. Satellite image products primarily from the HiRISE (high resolution imaging science experiment) sensor (McEwen et al., 2007) (Section 3.2) serve as large-scale overview and provide the spatial reference. For their use in 3D visualization tools, they are converted to meshes or Ordered Point Clouds (OPCs, see Section 5.1.2). They are also used for vision-based localization. Their primary data presentation tool is CAMP, the Campaign Analysis Mapping and Planning tool. CAMP is a web-based geographic information system (GIS) designed to support science operations (Abarca et al., 2019) and is built from the NASA AMMOS (Advanced Multi-Mission Operations System) GIS (Calef, Soliman, et al., 2021; MMGIS, 2022).

3. IDS 2D image processing (Section 4.2) applies radiometric and geometric correction to the images and combines images to mosaics. This is complemented by dedicated 2D image processing provided by the Mastcam-Z Team.
4. The Mastcam-Z Team employs its own radiometric calibration pipeline, using the results of the pre-flight calibration (Hayes et al., 2021) to convert raw images in units of observed Digital Number (DN) to average in-band radiance, removing detector bias, applying flat field and bad pixel map corrections, and, by multiplication, converting DN to radiance for a given filter/zoom combination.
5. IDS also provides 3D vision processing from individual stereo image pairs (Section 4.2).
6. PRoViP is a 3D vision processing chain for Mastcam-Z tactical use (Section 4.1). Its primary output is a repository of OPCs.
7. The ASTTRO Landform Toolkit (Section 4.3) combines images from various Rover instruments into a structure-from-motion chain, primarily for close-range applications to give the Mars 2020 tactical teams spatial context from the engineering point of view. It gains textured meshes that are presented and analyzed in its own 3D visualization tool (Section 5.3).
8. Structure-from-motion is also applied in science context, producing 3D descriptions of the rover's environment in multiple scales from images of various instruments and is the primary source to be presented on public channels such as Sketchfab.
9. Mission-internal data are available in a Planetary Data System (PDS)-compatible repository. This is regularly validated and deployed for public use. The primary access point in mission context is the mission's primary image viewing tool Marsviewer (Marsviewer, 2022).
10. PRo3D (Section 5.1), is a tool for real-time 3D visualization and analysis of large data sets in various scales (Barnes et al., 2018). It is fed by OPCs as generated by PRoViP from rover images and HiRISE DTM (Digital Terrain Model)/Ortho images. Its video rendering engine enables easy assembly of videos such as flyovers, documentation of geologic annotation and as discussion basis for long term planning.
11. Viewpoint (Section 5.4) is a 3D tool used by camera operators and science team members to plan imaging observations.

All the listed tools and data are available to the Mars 2020 Team (science and engineering), and some are deployed to the general public, see Text S9 in Supporting Information S1 for more information on categorization and specific features of the respective frameworks.

The selection of access points and “users” visualized in Figure 1 is only a representative subset.

### 3. Mastcam-Z and Related Image and 3D Data

Mastcam-Z is an important context-providing instrument with 3D capabilities, briefly characterized in the next subsection. Its counterpart on more global context is satellite imagery, which is briefly mentioned in the follow-on Section 3.2. Note that rover imaging strategy and products substantially differ from satellite imaging. This includes observation direction (shallow in most cases of rover imaging vs. almost perpendicular views in the satellite case), time-of-day with differing illumination/shadowing situation in the rover case, variation of pixel resolution across rover images in various orders of magnitude across a single image, different occlusion situations, influence of rover shadow and occlusions by rover assets, varying focal length and focus on the Mastcam-Z instrument and different degrees of freedom in radiometric response.

#### 3.1. Mastcam-Z Stereo Image Data Sets

Mastcam-Z is an identical pair of multispectral, 4:1 zoomable, focusable charged-coupled device (CCD) cameras (Bell et al., 2021), which provide color stereo views of the scene around the rover. The instrument's imaging sequences consist of one or more monoscopic or stereoscopic images in one or more spectral channels (including RGB from their built-in Bayer pattern), depending on the science intent posed for the respective sequence. For 3D data exploitation, such sequences are typically RGB stereo image sets. Hereby, stereo is either gained from the so-called “BOTH” configuration (meaning, using the calibrated fixed stereo imaging geometry without any motion between them), by re-pointing one of the cameras by a slightly different pan setting to increase the stereo overlapping geometry, or a combination of them.

Similar to the navigation camera (Navcam; Maki et al., 2020), as well as Supercam (Wiens et al., 2021), the Mastcam-Z cameras are mounted on the Rover Remote Sensing Mast (RSM) that is equipped with a pan-tilt



ability to direct the camera boresights with accurate to almost the entire spherical space around their rotation center. These additional two degrees of freedom are embedded in the instrument's geometric calibration (Hayes et al., 2021).

### 3.2. Context From HiRISE DTM/Ortho Image Data Sets

The data interpretation and analysis profits from the knowledge about large-scale context, in particular if combinations from 3D data obtained from different rover positions are concerned. The main source for 3D context is a DTM overlain with RGB or monochrome texture covering Perseverance's operational site (Ferguson et al., 2020). Its DTM, assembled by USGS (United States Geological Survey), has a spatial resolution of 1 m, complemented by a 25 cm-resolution monochrome texture layer, with an RGB part of the Ortho image, provided by the JPL Mars 2020 Science Team's mapping experts, in same spatial resolution of 25 cm. This DTM/Ortho combination is available both within CAMP (Section 5.2) and PRo3D (Section 5.1), yet only for the mission team, a publicly available version exists with monochrome texture layer ([https://astrogeology.usgs.gov/search/map/Mars/Mars2020/JEZ\\_hirise\\_soc\\_006\\_DTM\\_MOLA\\_topography\\_DeltaGeoid\\_1m\\_Eqc\\_latTs0\\_lon0\\_blend40](https://astrogeology.usgs.gov/search/map/Mars/Mars2020/JEZ_hirise_soc_006_DTM_MOLA_topography_DeltaGeoid_1m_Eqc_latTs0_lon0_blend40)). Figure S1 in Supporting Information S1 shows an overview of the OPC generated from the DTM, overlain with Perseverance's trajectory over the first 448 sols as displayed in PRo3D. All orbital images are tied to a Mars-co-registered areo-reference frame based on the MOLA (Smith et al., 2001) model. The RMS elevation amplitude in the flattest parts of the scene is on the order of 0.2 m (vertical), corresponding to 0.3-pixel matching error (Kirk et al., 2008). The Mars 2020 Navcam data is tied to the HiRISE via localization in 2D and 3D via manual image matching. Errors in Navcam data are further elaborated in (Abarca et al., 2019). The projection used for Jezero Crater is given in Text S2 in Supporting Information S1.

## 4. Mastcam-Z 3D Vision Processing Tools

This section focuses on the 3D vision processing and exploitation of Mastcam-Z stereo- and multi-stationary imaging. There are two pipeline-based processing entities that are used in a tactical context (i.e., processing fully automatic right after images' downlink receipt), namely IDS (Section 4.2) and PRoViP (Section 4.1). Although there is some overlap in what IDS and PRoViP do, they are generally complementary to each other in terms of their use. IDS products are certainly usable for science, but the first focus is on operations. IDS thus maintains a systematic pipeline that does all the same processing on every image that comes down, IDS also makes some special products manually, but the focus is on pipeline production in a rapid turnaround for operations use. PRoViP on the other hand is more science focused, making select products that are most useful for scientists and geological interpretation of the data, yet still in a tactical time frame and fully automatic. PRoViP and IDS mainly rely on the geometric calibration and Rover poses provided by the mission's localization team.

Another mission-embedded tool is the ASTTRO Landform Toolkit (Section 4.3) to generate meshes mainly used by rover drivers, and to enable target definition within its ASTTRO visualization frontend (Section 5.3). The Landform Toolkit uses SfM to obtain/refine camera poses and hence is flexible in terms of the combination of multiple instruments' data into the gained meshes. SfM is also used to generate publicly available meshes as for the Meshlab data generation workflow described in Section 4.4, allowing the public to browse and visualize Perseverance's surroundings interactively in 3D.

### 4.1. PRoViP: Planetary Robotics Vision Processing

Mastcam-Z stereo pairs enable the generation of 3D vision products (e.g., DTMs), textured meshes, mosaicked panoramas and derived products for visualization and quantitative 3D analysis of the terrain (Traxler et al., 2022). Individual image processing and stereo photogrammetry steps (Paar et al., 2016) use the instrument's geometric parameters, the known pointing RSM pan-tilt angles, and the rover poses provided by the rover localization team to assemble a set of 3D vision products to be used by further scientific assessment.

- Stereo matching establishes dense pixel-to-pixel correspondences between left and right images (hence parallaxes that contain quantitative hints for distance).
- 3D triangulation projects the parallaxes onto a gridded model of the subject's surface topography (e.g., an infinite virtual cylindrical or spherical space around the sensor).

- Image texture is projected onto a grid, using the same geometric relationships.
- Data from adjacent stereo patches are fused to create a mosaic for distance, texture, and 3D coordinates.
- An OPC is produced to allow efficient visualization of huge data sets.
- For the 2D mosaic case: Camera textures are projected onto a virtual (infinitely distant) sphere or cylinder, they are mosaicked using optimization to minimize visual artifacts between patches.

This functionality has been developed generically in terms of missions and instruments (Paar et al., 2022a). The 3D Mastcam-Z stereo-processing products are assembled tactically in a sequence of “processors” with a time frame of about 1 min per stereo pair, and made available as fused products (OPCs, mosaics, distance maps from entire pan-tilt sequences) in geographical coordinate frames to the Mastcam-Z and Mars 2020 Team via a dedicated sftp repository, a version of which providing access to those products stemming from PDS-released Mastcam-Z data (see the Data Availability Statement). A typical PRoViP processing workflow is listed in Text S3 in Supporting Information S1.

PRoViP builds upon radiometrically corrected “RAD” products, as made available as output of the Mastcam-Z-internal tactical radiometric processing chain on servers run by the Mastcam-Z PI Team at Arizona State University (ASU). The following high-level workflow has been realized.

1. Newly incoming images are detected on the ASU server, and uploaded onto a sftp server running at JR in Austria, together with an automatically generated PRoViP processing job description file and the latest rover localization information which is downloaded from a publicly available web page ([https://mars.nasa.gov/mmgis-maps/M20/Layers/json/M20\\_waypoints.json](https://mars.nasa.gov/mmgis-maps/M20/Layers/json/M20_waypoints.json)) maintained by the JPL rover localization team
2. A server process at JOANNEUM RESEARCH (JR) recognizes newly incoming Mastcam-Z data and launches processing of the newly received sequences
3. Science team members are notified by email upon finalization—including thumbnails and statistics of the completed jobs.

#### 4.2. IDS

The IDS is the Mars 2020-specific data processing division of the Multimission Image Processing Laboratory (MIPL) at JPL. IDS is responsible for processing all camera data and most data from non-camera instruments on the rover (which are not discussed further here).

IDS starts with the telemetry provided by the spacecraft and generates a wide variety of image products, for all the cameras on the rover and helicopter (Balaram et al., 2021), as discussed in overview form below. Table S1 in Supporting Information S1 provides a summary of the major IDS product types. Full details of the IDS system are available in (Ruoff et al., 2022).

IDS uses multimission software developed as part of the VICAR image processing system (Duxbury & Jensen, 1994). This software has been used on Mars Pathfinder, Mars Exploration Rovers (MER), Phoenix, Mars Science Laboratory (MSL), InSight, and now Mars 2020. It is based around a core set of C++ classes that encapsulate mission dependencies, wrapped in a wide variety of mission-independent and reusable application programs. As such, the products produced by IDS should be familiar to anyone who has worked with data from the prior Mars surface missions.

IDS is embedded in the operations cycle of the mission. IDS produces terrain meshes and orthomosaics that are used to plan rover drives and arm operations. It produces mosaics which are used by science and operations teams to understand the geological and operational context of the rover. It provides images and mosaics for Marsviewer, a primary team tool for viewing image data. It produces the raw image products that go into the PRoViP and Mastcam-Z processing chains, and which are made available to the public (NASA, 2022). It maintains a database of rover locations. It produces the bulk of the data that goes to the PDS archive, although science teams including Mastcam-Z contribute to the archive as well.

Figure 2 gives a high-level overview of the IDS image processing flow.

Concerning *single-image processing*, the first set of image products IDS produces are the raw products—the EDR (Experiment Data Record) family of products. These have minimal processing, reconstructing telemetry into a usable image format with metadata labels, and then doing minor image reformatting such as decompanding and

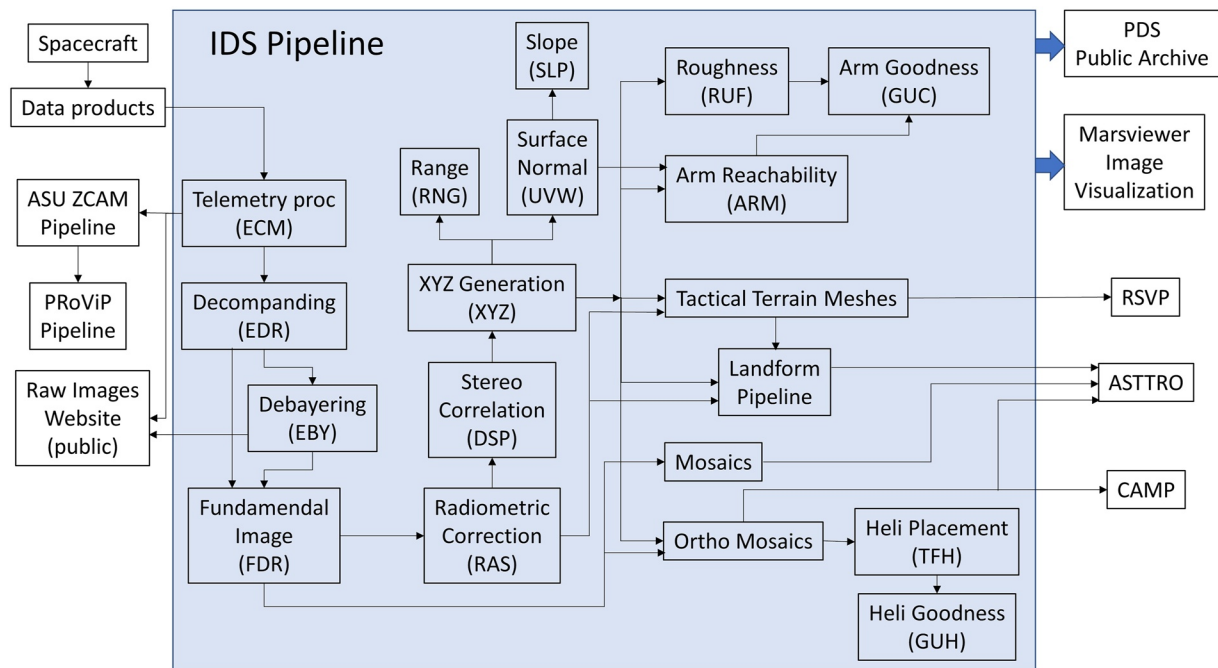


**Figure 2.** Main parts of Instrument Data System data flow. The acronyms of individual products (ECM, EDR, EBY, FDR, RNG, SLP, UVW, XYZ, DSP, RAS, RUF, GUC, ARM, TFH, GUH) had been selected for uniqueness purposes and are reflected in the file names of the respective products, see the Software Interface Specification (Ruoff et al., 2022), and the list of acronyms at the end of this paper. RSVP, Robot Sequencing and Visualization Program.

de-Bayering: Most Mastcam-Z images are “companded” (compressed in dynamic range from 12 to 8 bits using a square-root encoding table). Decompaning restores them to the original 12 bit linear response. De-Bayering is the process of converting a Bayer-pattern-encoded image to color using the Malvar algorithm (Malvar et al., 2004). These products form the basis of the PRoViP and Mastcam-Z processing chains, and are sent to the public immediately via the raw images web site.

Higher level processing then produces several forms of RDRs (Reduced Data Records).

Various forms of radiometric correction remove instrument effects such as camera vignetting. Although not as extensive as what the Mastcam-Z team does (e.g., IDS uses a single set of calibration data, which does not vary based on analysis of the cal target), it is within a few percent of the full science radiometric correction. A partial photometric correction (“zenith correction”) compensates for the solar intensity based on elevation and (optionally) atmospheric tau.

Mosaics are a very important part of 2D processing. Mosaics are systematically produced in several projections: cylindrical, polar, vertical (overhead without layover correction), orthorectified (overhead with layover correction), and stereo panoramas (cylindrical-perspective hybrid). Cross-instrument mosaics are also produced, such as RMI (Remote Micro-Imager)-over-Mastcam-Z (Figure 4).

*Stereo image processing* is the core of what IDS does, forming the basis of the terrain meshes used by the Rover Planners (RP) and ASTTRO to decide what to do, plan the commands, simulate the results, and ensure that the rover will be safe and do what was intended.

Stereo processing starts with image correlation. This is a process of finding, for each pixel on one image, the corresponding pixel on the stereo partner image (e.g., left vs. right). The process uses an affine projection (optionally plus xy terms) to compensate for the different view geometry of the two eyes, and then uses a standard cross-correlation coefficient measurement to find the best match for the region around the pixel (Deen, 2003).

From there, XYZ coordinates for each pixel are obtained by projecting the results through the camera models for each eye and looking at their intersection in space. A range filter step reduces noise in trade-off with spatial resolution. These XYZ data (also visualized in color, see Figure 3) are the fundamental basis for the remaining products, optionally masked to remove rover parts.



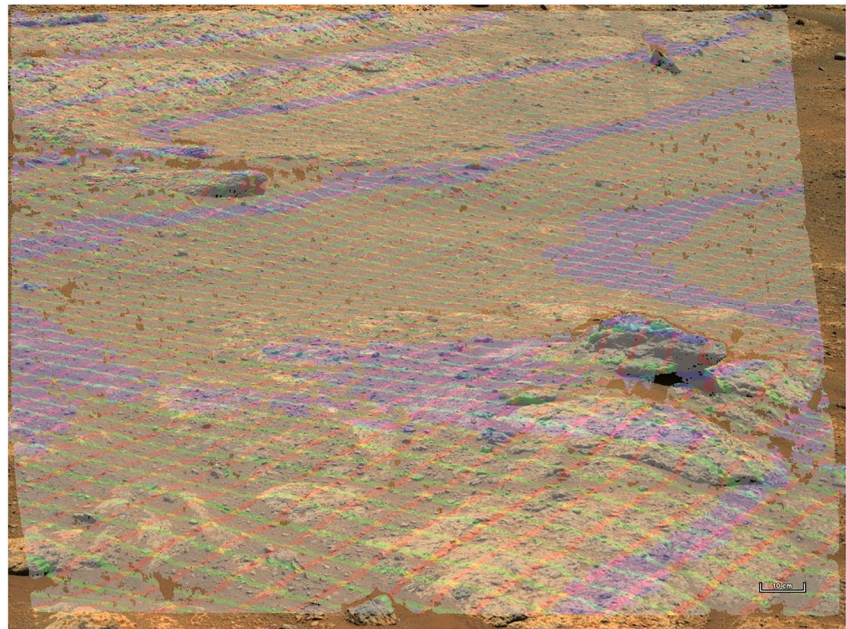


**Figure 3.** xyz information (xy grid 10 cm spacing, z color-coded with blue = isoline 10 cm of height w.r.t. rover wheel bottom) overlain on a 34 mm Mastcam-Z image from Sol 163 with the sequence id ZCAM08172. Note the scale bar at bottom right, being adequate in size when looking at the image on a 4k (Ultra-High-Definition) resolution screen.

The XYZ's are converted to surface normals using a plane fit, and from there to slope images of various kinds, which indicate where it is safe for the rover to operate. An important visualization product is an orthomosaic, see Figure S21 in Supporting Information S1.

XYZ's are also used to make reachability maps. These show where in the image the robotic arm can reach, and in what configuration. Roughness maps show whether it is safe to obtain a core sample, with overall goodness maps combining all that information for arm operators. Similar maps were created for the first helicopter operations, to assess safe landing zones.



**Figure 4.** Overlay of Remote Micro-Imager images (recognizable circular footprints) over a Mastcam-Z mosaic from Sol 150, Sequence 3188. The image shows rocks of the Máz formation on the Jezero crater floor with surfaces that were modified by wind abrasion.



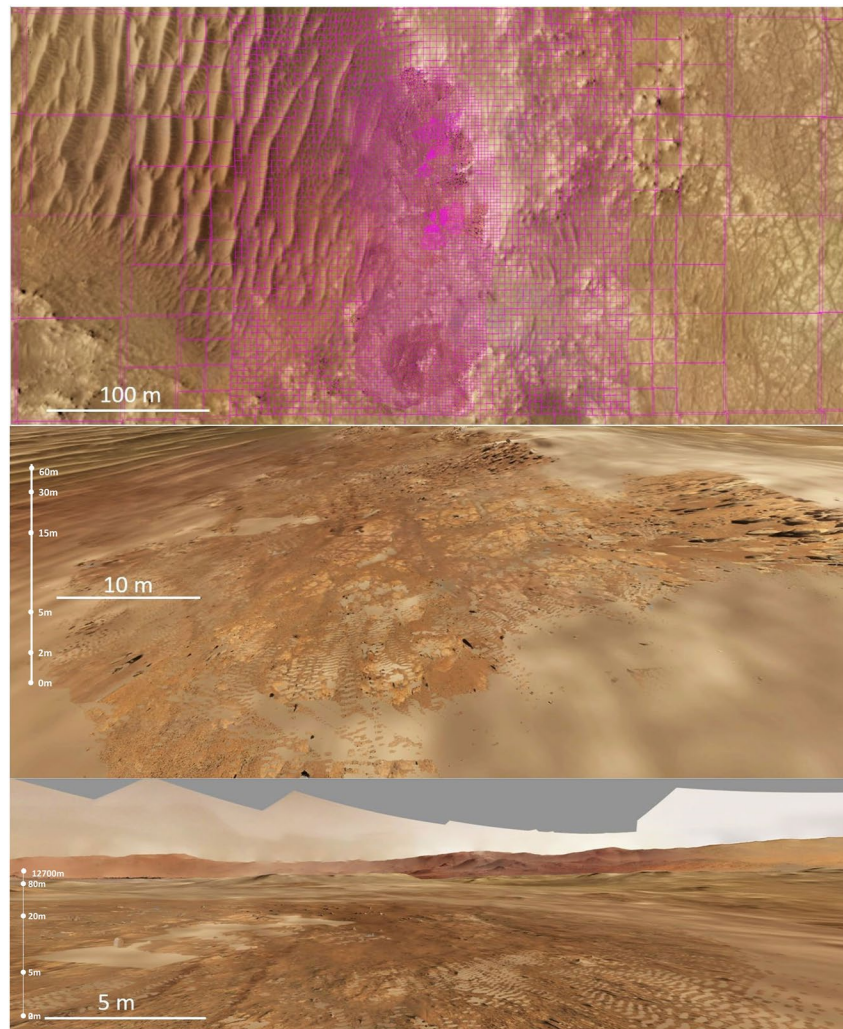


**Figure 5.** (Top) 3DTiles tilesets break up large meshes for hierarchical on-demand streaming (Sol 153). Landform adaptively creates finer tiles in areas with higher available detail. (middle) the contextual mesh combines high-resolution local surface observations with broader but coarser orbital data (Sol 153). (bottom) a sky sphere showing the horizon can improve spatial awareness (Sol 153). Scale bars are approximations and apply to the location of their placement.

The most important derived 3D product is the terrain mesh. This is the result of decomposing the XYZ image into triangles that geometrically define the surface. This mesh is ultimately what the RPs and ASTTRO users interact with to command the rover.

### 4.3. ASTTRO Landform Toolset

IDS includes several systems to generate terrains subsequent to 3D vision processing. One of these, called Landform, produces 3DTiles (Cozzi et al., 2019) tilesets for the mission science tool ASTTRO (see Section 5.3). Landform both converts each stereo camera “wedge” to a tileset and also produces much larger orbital and contextual tilesets. The 3DTiles format breaks potentially large meshes into a hierarchy of tiles (see Figure 5, top) which are streamed as needed to a web client running the ASTTRO application. The quadtree-like hierarchical decomposition enables web-based viewers such as ASTTRO to navigate potentially large terrain data sets using limited client-side CPU and memory resources, and without waiting for long downloads due to limited network bandwidth. When the viewer is zoomed out only several tiles from the coarse level of the hierarchy are loaded. Conversely, when the viewer is zoomed into a specific region of the data set, only a subset tiles from the finer levels of detail for that region are loaded. A user may view either a collection of tactical wedge tilesets (up to hundreds simultaneously, e.g., for large Mastcam-Z panoramas), a kilometer-extent orbital tileset, or a contextual

tileset that fuses data from up to thousands of surface observations with orbital data, providing spatial awareness for science planning (NASA, 2022). Landform automatically produces new tilesets whenever data becomes available using an AWS (Amazon Web Services) cloud deployment with multiple servers that process data in parallel.

The contextual tileset pipeline is the most significant part of Landform. It automates the large task of aligning data from multiple rover positions together and to orbital data, reconstructing kilometer-scale terrains with both coarse orbital regions and finely detailed surface-data areas (see Figure 5, middle). It also combines surface and orbital imagery to texture the terrain and creates a sky sphere to show features on the horizon. Landform differs from other photogrammetry and SfM systems in that it leverages properties of mission data such as the availability of good pose priors, stereo vision, calibrated cameras, and orbital data. These can enable relatively reliable automated processing compared to generic tools not specifically adapted for this case. Each contextual mesh can take up to about 4 hr to produce on a 72-core server, with processing comprised of six phases.

1. *Ingestion*: Landform automatically scans mission databases to collect stereo vision point clouds and visual images from each new rover location as well as previous data from nearby locations. Up to hundreds of stereo camera point clouds and thousands of images may be collected.
2. *Alignment*: Observations taken from the same rover position are often already well aligned to each other. However, alignment of data across rover positions may be more noisy. Landform applies a custom feature-matching “birds eye view” aligner to improve alignment across rover locations, followed by an iterative closest point algorithm to align surface to orbital data.
3. *Mesh reconstruction*: Poisson surface reconstruction (Kazhdan et al., 2006) is applied to the aligned point cloud data in a local detail region and the result is sewn into a larger coarse mesh derived from orbital data. The full mesh may have up to around 100M triangles and several kilometers of spatial extent. It is broken into an adaptive grid of leaf tiles for further parallel processing.
4. *Texturing*: a texture image is formed for each leaf tile with a backprojection algorithm that selects pixels from the best available surface images, falling back to orbital imagery where necessary. A multigrid algorithm (Kazhdan et al., 2010) is applied to reduce seam artifacts.
5. *Hierarchical LoD (Levels-of-Detail)*: A hierarchy of parent tiles is created by recursively combining and simplifying finer tiles using floating scale surface reconstruction (Fuhrmann & Goesele, 2014).
6. *Sky Sphere*: A separate tileset is created with hemispherical geometry surrounding the terrain. The same texturing algorithm is applied to paint surface imagery onto the sky sphere, with some modifications to mask features that are already visible in the terrain (Figure 5, bottom).

#### 4.4. COTS (Commercial-Off-The-Shelf) Tools Applied for Structure From Motion

Structure from Motion (SfM) is a more general form of the stereo processes discussed above. The applications of 3D models made from SfM are similarly compatible to the tools discussed above while also enabling new applications. State of the art SfM photogrammetry has advanced considerably in the past decade to the point that several commercial Software packages can produce scientific data products with several advantages over the specialized process commonly used in planetary science. A few COTS or even open source/open access tools have emerged for stable use—commercial software was used in the solution and cases here, because its quality in experiments with Mars 2020 images turned out to be significantly greater than that of the open-source competitors.

The advantages of using SfM in modeling the Martian terrain are twofold. First, SfM can fuse more images and perspectives than the two images of a traditional stereo pair, and second, SfM optimizes the camera parameters to mitigate errors in the camera's calibration, pointing, and localization. The SfM workflow used in this work is explained in Text S4 in Supporting Information S1.

Figure 6 shows the workflow after the images and metadata are loaded into Agisoft Metashape Professional, with the result available under Sketchfab on <https://skfb.ly/o7vUP>. Some further results demonstrating the ability of change documentation and analysis are shown in Figure S20 in Supporting Information S1, and, with a virtual model of Perseverance, Figure 7.

Various types of SfM models can be made with the rover data set, from proximity science footprint (0.1-m square), workspace models (1-m square), medium range models from two or more short drives (10-m square), and long-range models of targets more than 100-m distant from at least two distant rover positions, also called “Long Baseline Stereo—LBS,” as the fixed stereo baseline between the Mastcam-Zs becomes negligible at large



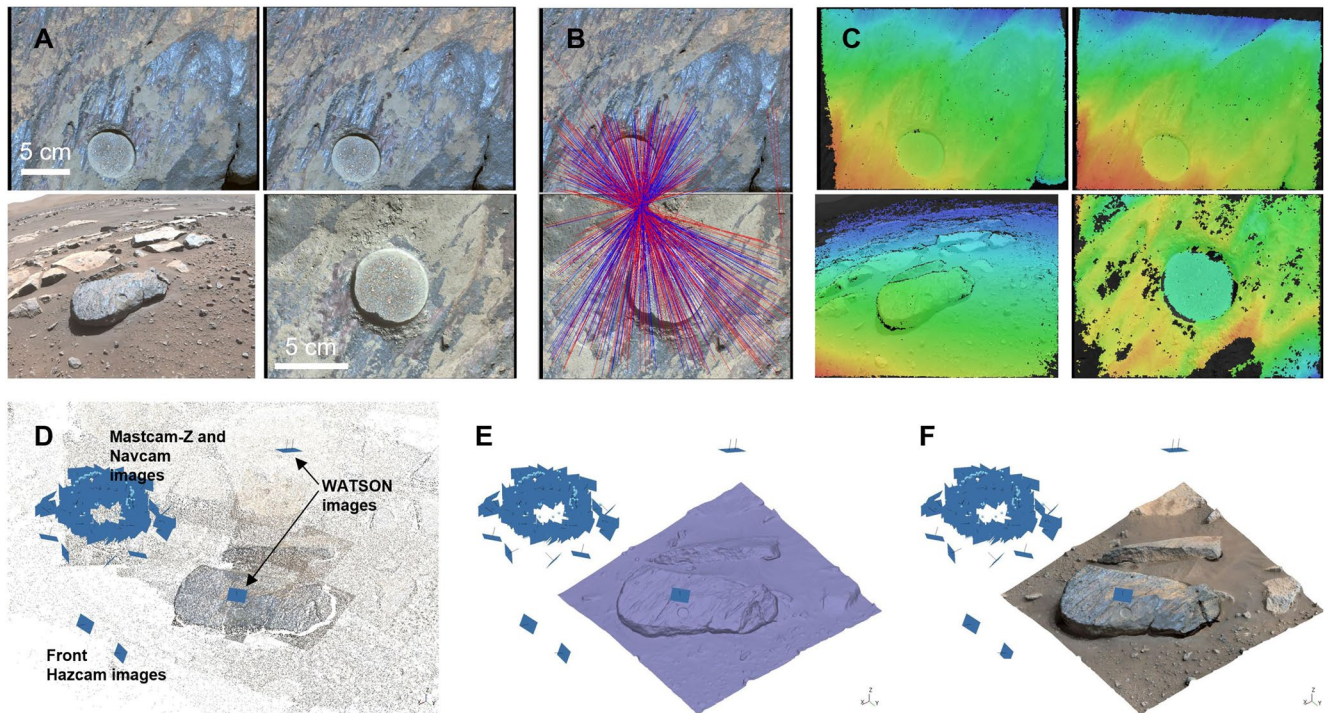


**Figure 6.** Example of Structure from Motion using the “Rochette” rock which was a target for sampling of two drill cores in September 2021, with images taken between Sols 185 and 194.

distances (>1 km) and can no longer produce reliable models. In the LBS case, normally only one of two stereo partners are used from each rover location, since the additional stereo partner would not add much additional information.

- (A) Four images used in the 3D reconstruction. The top-left and top-right sub-panels are Mastcam-Z images at zoom focal-length 110 mm. The bottom-left is a high-resolution right Front Hazcam, and the bottom-right is a high-standoff WATSON image on the rover's robotic arm.
- (B) Tie-point matches between right Mastcam-Z and WATSON images. The blue lines connect valid matches, while the red lines are rejected to avoid incorrect matches. At this orientation, the WATSON image is roughly upside down relative to the other cameras.
- (C) Depth-maps for the images in (A) generated from the fine-scale matching between the valid tie-points as (B).
- (D) View of the scene from above and to the right of the rover. Blue rectangles are aligned cameras, and the colored dots are valid tie-points.
- (E) 3D reconstruction from the depth maps in (C).
- (F) Textured model blended from the original images in (A).

## 5. Mastcam-Z 3D Data Presentation Tools

### 5.1. PRo3D: 3D Real-Time Multi-Scale Immersive Visualization and Analysis

#### 5.1.1. PRo3D Scope

The Planetary Robotics 3D Viewer, in short PRo3D (PRo3D, 2022), is an open-source interactive 3D visualization tool that allows members of the Science and Operations teams to work with high-resolution 3D reconstructions of the Martian surface (Barnes et al., 2018). 3D reconstructions may stem from a variety of camera instruments capturing images either from orbit or from the ground-level. The key requirement is to view and analyze these data together in their common geospatial context. As described in Section 4, PRoViP performs the necessary transformations while PRo3D allows users to browse 3D surface reconstructions ranging from kilometer to micrometer scale.

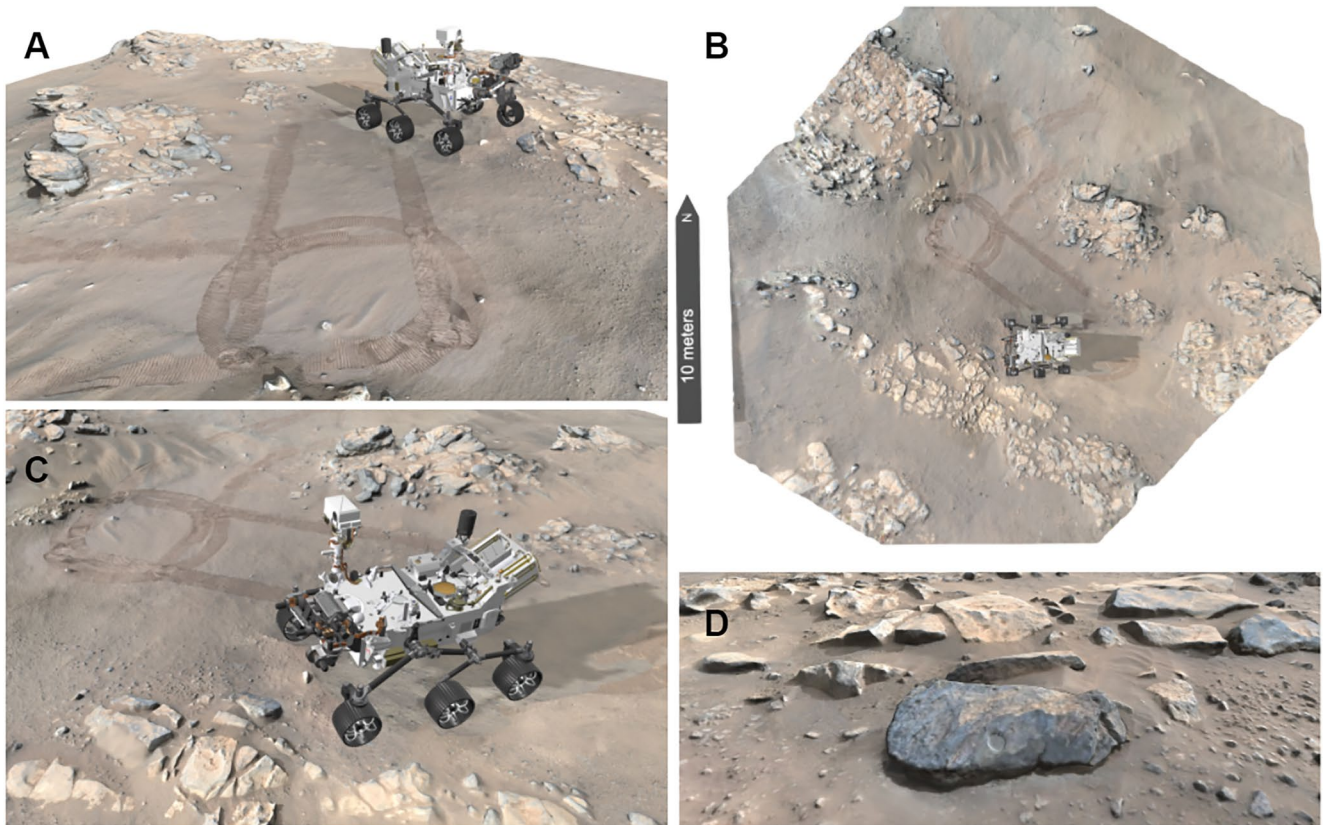


**Figure 7.** A 3D model view in Sketchfab <https://skfb.ly/opQMQ>. This example is made with Structure from Motion (SfM) from images of the Citadelle site and Rochette rock on Sols 180–198. (a) Side view heading northeast with a model of Perseverance Rover to scale relative to the landscape (b) Top view with North up and a scale-bar for 10 m. (c) Side view heading northwest. (d) View of Rochette approximately from the perspective of the Front Hazcams.

We address this requirement by meeting two design goals: First, PRo3D needs to cope with large scale orbiter DTMs and multiple high-resolution rover reconstructions that can easily lead to gigabytes of geometric and image data, and second, PRo3D handles multiple representations at different resolutions for the same region on Mars in a flexible and comprehensible way. It is also being used as a 3D GIS.

Further PRo3D aspects are explained in more detail in Text S5 in Supporting Information S1.

### 5.1.2. Geological Annotation and Analysis Tools

The initial use case for PRo3D was to support planetary geologists with tools to conduct remote geological analysis on 3D digital outcrop models, that is, 3D surface reconstructions mostly from science cameras. However, the suite of measurement tools can also be employed to serve operational use cases, for example, judging distance, height, and steepness of terrain to be traversed. All measurements are based on the interaction of the user clicking on the screen which spawns a ray pointing into the 3D scene. This ray is then intersected with the 3D surface geometry of the highest available detail, that is, level 0, typically consisting of millions of triangles. To reduce computational load we sort the triangles into a *kd-Tree*, a spatial acceleration data structure that allows us to exclude a large number of triangles from being tested for intersection. Further, we also need to employ an out-of-core loading strategy that loads *kd-Trees* on-demand. The resulting points on the surface can form single point, line, polyline, and polygon annotations. We compute a series of measurements for each annotation, such as length or bearing and also allow users to add arbitrary text displayed as 3D billboards facing the screen. To convey semantic information, annotations can be styled by color and thickness.

PRo3D currently offers two tools specifically designed for conducting remote geological analysis. The first, dip-and-strike is essential for judging orientations of strata and cross-beddings. The users pick points on the surface forming a polyline, while on completion we use a PCA (principal component analysis) based method, as shown by (Quinn & Ehlmann, 2019), to fit a plane to the respective positions. PRo3D also computes and displays



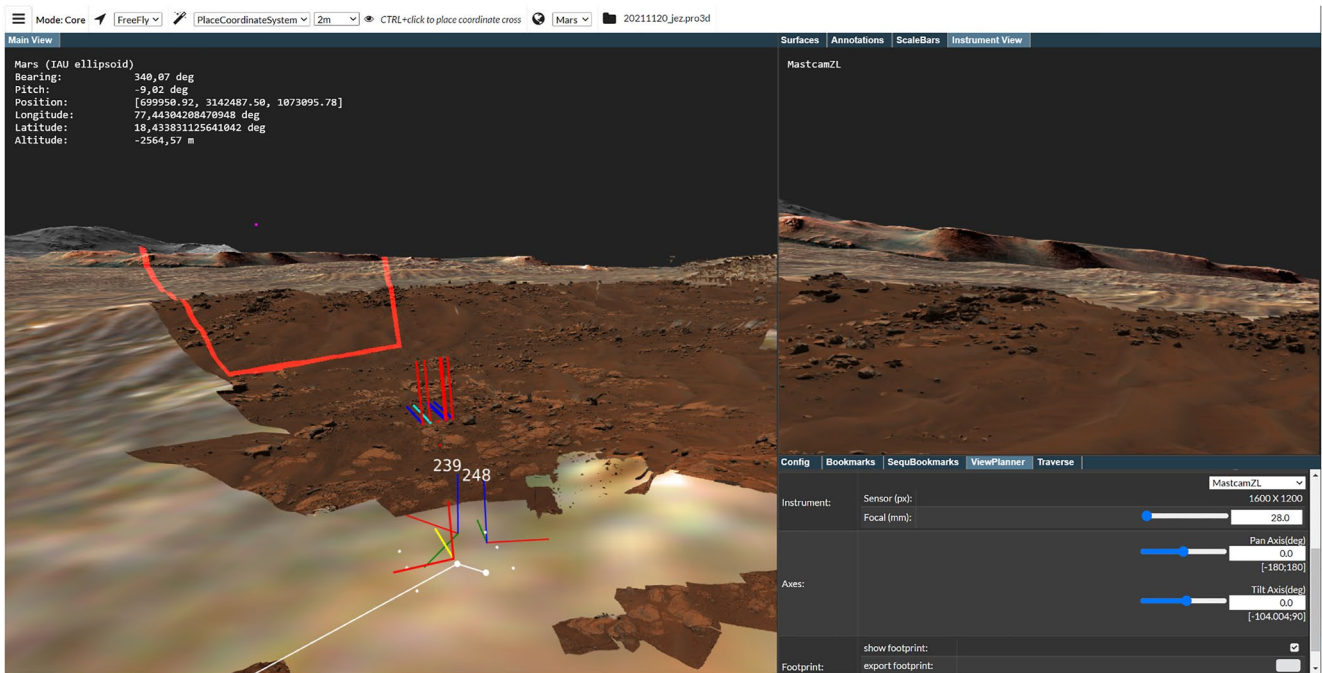


**Figure 8.** Planning a view for the left Mastcam-Z of the Perseverance Rover. The camera instrument parameters such as pan and tilt angles are adjusted in the Graphical User Interface panel (bottom right), the corresponding instrument footprint is shown in the 3D view (left) as red polygon together with an abstract rover model, the simulated view is rendered into the upper right frame (© NASA JPL/ASU/JR/VRVis), HiRISE data: USGS (DTM & panchromatic Ortho layer) and JPL Mars 2020 Science Team (RGB Ortho layer).

the suggested radial error metrics to judge the robustness of the fitted plane. The second is the “true thickness” tool where users connect two points with a line and further manually specify dip angle and dip azimuth to estimate the true thickness of strata, opposed to their apparent thickness. As in-depth geological interpretations may contain thousands of annotations, PRo3D offers a GUI (Graphical User Interface) to sort annotations hierarchically into named groups. To carry over measurements taken in PRo3D to other tools we offer a variety of export methods, such as CSV (Comma-Separated Values) or GeoJSON (Geospatial JavaScript Object Notation), making use of IAU-Mars coordinate space (IAU-2022), with coordinates being translated to geographic coordinates in real-time in the GUI using the SPICE Toolkit (SPICE, 2022).

See Figure 17 for an example of a PRo3D-based outcrop interpretation in the scope of the Mastcam-Z mission.

### 5.1.3. PRo3D View Planner

The View Planner is a tool integrated into PRo3D. It helps to optimize image capturing positions and parameters for a rover camera instrument and perform visibility analyses (Traxler et al., 2017). View planning starts by placing the rover onto a desired surface position. For that, mainly reconstructions from orbiter imagery are used. Higher resolution DTMs from rover imagery can be considered if available, for example, to plan further observations of the corresponding site. The rover and its instruments are represented in an abstract way by dots and lines. Next the operator chooses a camera instrument in the GUI and adjusts its parameters such as the pan and tilt angles and the zoom factor. The instrument footprint, which is the visible area for a particular setting, is visualized by a red polygon (see Figure 8). Additionally, a simulated view of the camera instrument is shown in a separate frame. Both the polygon of the visible region and the simulated view are updated in real-time when the operator changes the instrument settings. This highly interactive and geospatially accurate approach allows one to efficiently find optimal viewpoints and camera settings.

### 5.1.4. PRo3D Bookmarks, Traverse Integration, and Video Production

PRo3D allows users to trigger an automatic fly-to animation to any object in the 3D scene. For this we compute a camera animation path to smoothly transition between the current view and the characteristic view of the respective target object. Users can also define and name so-called “bookmarks”, essentially describing the current view

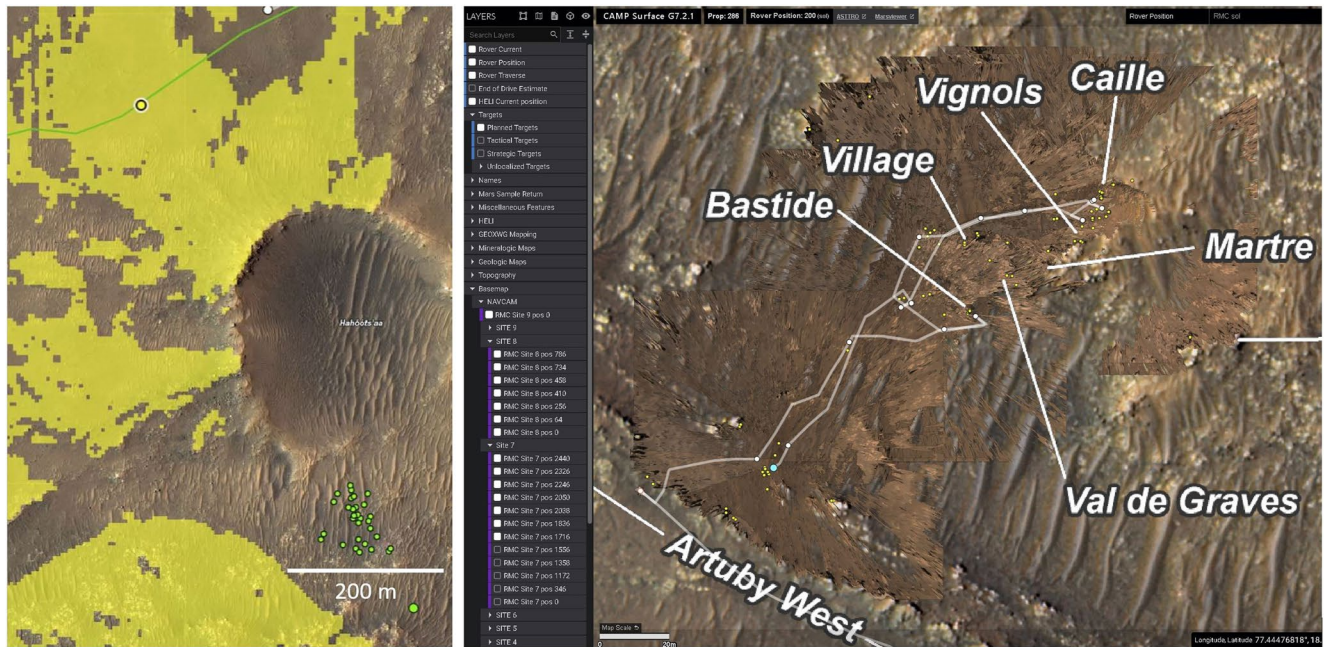


**Figure 9.** Left: Campaign Analysis Mapping and Planning (CAMP) Viewsheds near the rover traverse. The white dot indicates the position of the rover on Sol 400. The large subrounded feature on the crater floor is the impact crater Hahótsaa. Right: CAMP annotations showing the rover traverse as well as outcrops and targets of the Séítah formation (Bastide, Village, Vignols, Caille, Martre, Val de Graves) and the Mááz formation (Artuby West).

by position, orientation, and field of view, which can be traveled to in the aforementioned way (Paar et al., 2022b). We discovered that users tend to use bookmarks as a means to tell stories about their data and analysis, so we added sequential bookmarks. This interface allows users to arrange these 3D frames in a linear way and jump between them in sequence in real-time while concentrating on the narration rather than on navigation. Animation durations and delays can be defined, and further still-frames can be rendered during automatic playback to efficiently transform a scene into a high quality video, see various examples available on the PRo3D YouTube channel <https://www.youtube.com/channel/UCIigAd9TIn0NdJ1MB6iW5Nw>.

The individual Sols of the rover's traverse are essential to contextualize data products and scientific insights. Therefore, PRo3D supports the ingestion of the Mars 2020 traverse in GeoJSON format visualized as a white poly-line, where each vertex is labeled with the respective Sol number. As each Sol contains information about the rover pose, a fly-to animation to the respective Sol puts the current view into the exact location and orientation of the rover at this time. Sols are also integrated with the “viewplanning” functionality allowing the users to create a viewplan from a specific rover pose.

## 5.2. CAMP—A 2D and 2½ D GIS

The Campaign Analysis Mapping and Planning (CAMP) tool is built from the NASA AMMOS Multi-Mission GIS (MMGIS) (Calef, Soliman, et al., 2021), which provides part of a spatial data infrastructure in the form of capabilities to display and analyze geospatial data sets. MMGIS is a free and open source software for geospatial (FOSS4G) web-based framework for planetary missions. The software has been/will be deployed or used by four active (InSight, MSL, Mars2020, Mars Helicopter) and four future (Mars Sample Return, ESA Rosalind Franklin rover, Lunar VIPER rover, AEGIS) planetary surface missions as well as two Earth-based projects. CAMP can display data as both 2D maps and 3D, though because it focuses on orbital data sets for elevation, maps are displayed in 2.5D (i.e., no overhangs or true cliffs). For Mars2020, CAMP provides situational awareness of the rover position, access to multiple science team derived maps, and the ability to record areas of interest for strategic planning. For the engineering team, these strategic science maps are used to estimate future drive positions and make assessments of current resources versus mission progress along a strategic path over time. Geospatial data typically displayed in CAMP include.

- Orbital basemaps and elevation models.
- Science team geologic and spectral maps.
- Rover in situ imagery as orthophoto mosaics.
- Science targets, both in tactical and strategic (= across various rover positions in weeks' or months' time frame).

These data sets are either pre-tiled in TMS (Tile Map Service) tile format (raster data sets) or served as GeoJSON (vector data sets). Elevation data is also tiled in a special tile format that replicates the above TMS structure, but encodes 32-bit data into an 8-bit format. Tactical science targets, those used for pointing instruments, are localized by knowing the rover position on the basemap, then adding that to the relative position of the target from the rover. Strategic science targets, those areas of interest, are created directly in CAMP on the existing basemap.

The software and data is deployed in a cloud architecture (AWS, Simple Storage Service [S3], Elastic File System [EFS]) which allows scaling both instances and data volume. CAMP is always accessed by a WebGL (Web Graphics Library) capable web browser to enable all capabilities, both 2D and 3D. The main tools used by the science team include.

- Measure tool: provides estimates of distance, azimuth, and elevation profile.
- Viewshed tool: shows what areas are visible on the landscape around the rover based on current or future rover positions or for different instrument FoV—see Figure 9, left, for an example.
- Draw tool: allows science team members to share areas of interest and operations to develop, and share, a strategic plan with the whole mission.

The science team uses the above tools to help find distances to far away targets (see Figure 9, right, for an example), estimate viewable outcrops from potential rover positions, and record areas of scientific interest. The 2.5D capability has also been exploited by RP to assess upcoming terrain and provide a “strategic path” that has can be traversed by the rover.

### 5.3. ASTTRO 3D Visualization

The ASTTRO is a web-based application that gives the Perseverance rover science team situational awareness of the rover's position, kinematic state, and surrounding terrain (Abercrombie et al., 2019). ASTTRO includes a three dimensional interactive visualization of the rover and terrain, as well as 2D visualization of rover images. ASTTRO can visualize several types of data.

- 3D models derived from the MastCam-Z instrument.
- 3D models derived from the Navigation or the Hazard camera images.
- Orbital mesh from the HiRISE instrument.
- A contextual mesh product that combines the above sources to produce a mesh that optimizes texture resolution using a fusion of data sources.

The 3D ASTTRO rendering engine displays mesh products processed by the Landform tools (Section 4.3). These products are provided in the 3D Tiles format. These data are downloaded from the Amazon Web Services Simple Storage Service (S3), and rendered directly in the web browser using WebGL. Landform (Section 4.3) produces several levels of detail, which are described as a data hierarchy in the 3D tiles format. This format provides the metadata necessary for the rendering client to download only the tiles necessary to render a given view, and with an appropriate level of detail for the display.

The primary functions of ASTTRO are to help the science team understand the orientation and the kinematic state of the rover relative to the surrounding terrain, and to visualize the position and orientation of “targets” created by the science team (Figure 10). A target is a named point in space identified by cartesian coordinates, azimuth and elevation, or pixel coordinates in a reference image. Targets are used for instrument pointing to acquire new observations. ASTTRO is also the primary tool used to create new targets in the mission target database.

ASTTRO also provides features to help the science team check instrument constraints to determine if a given target may be observed. For example, instruments mounted on the turret of the robotic arm must be able to reach the target (in a kinematically possible arm position), and may also have constraints on the properties of the target surface (e.g., roughness). Remote sensing instruments may have range constraints, or lighting constraints.



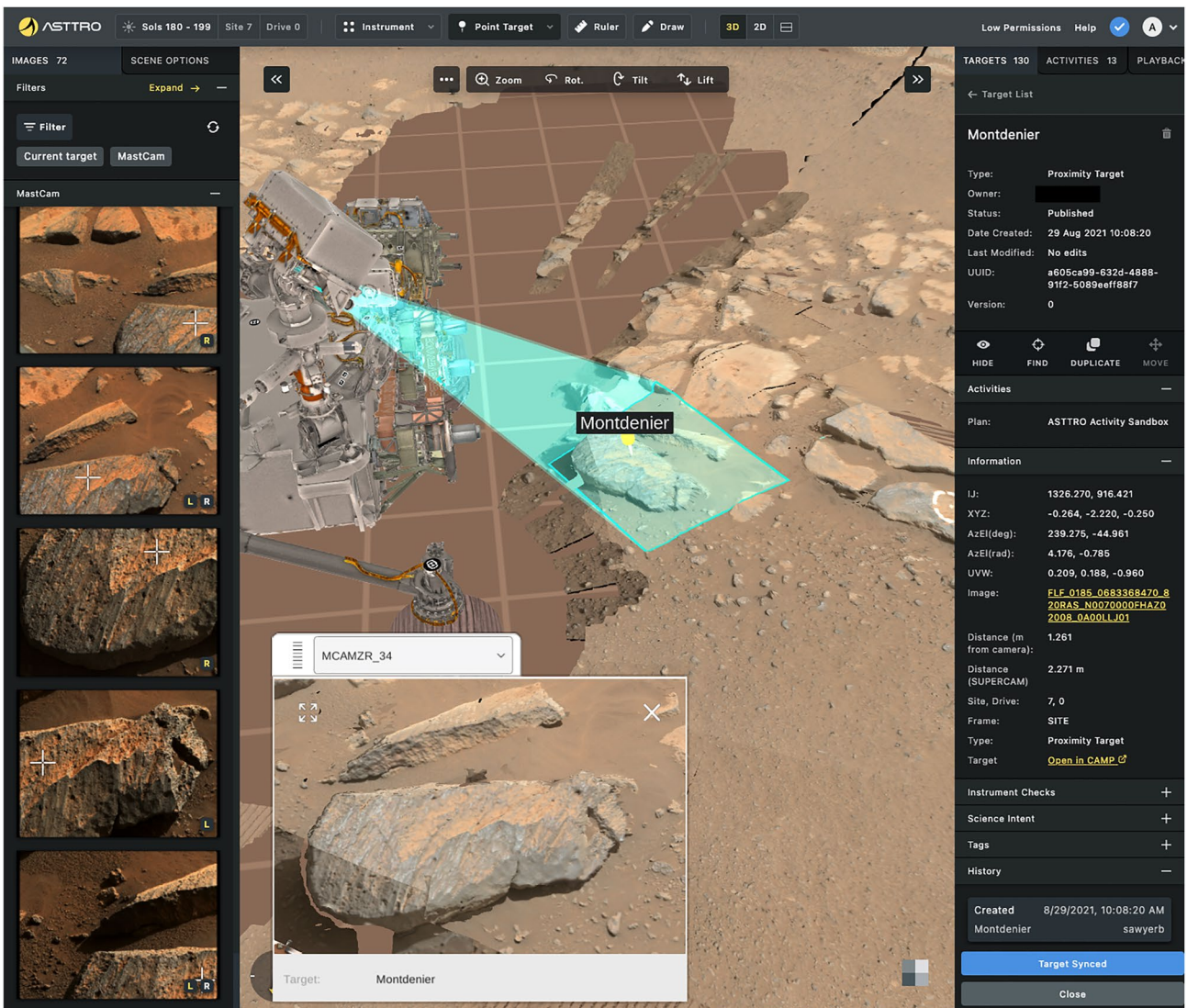


**Figure 10.** Advanced Science Targeting Toolkit for Robotic Operations rendering of the Mastcam-Z terrain wedges to prepare the sample drilling process at Rochette, produced by the Landform tool, using data between Sol 180 and 199. White crosshairs in the image gallery on the left show the position of the selected target called “Montdenier.” The tool also shows the footprint and preview of a Mastcam-Z image of this target for the 34 mm zoom setting. The underlying grid is sized 1 m, rendered 2 m below the main surface level.

ASTTRO includes sun and shadow modeling to help the team understand the impact of lighting conditions and shadowing on observations (ASTTRO simulates shadows for a predicted sun direction using the Unity graphics engine real-time shadowing rendering feature. This rendering system uses shadow maps rather than a physically based BRDF). Ingestion of the HiRISE textured mesh provides context for the surface image mesh by allowing the user to see a greater spatial extent around the rover (Figure 11).

In addition to 3D visualization, ASTTRO can also display rover images (both single frame images and mosaics). The software includes a 2D/3D correlation feature that can translate points from a 2D image to the 3D view and from 3D back to 2D. In addition, the tool can find all images that include a selected 3D point, allowing users to easily find related views of a feature. This is especially useful to locate additional views of a context image that covers a small spatial scale (e.g., from the SuperCam remote imager, Wiens et al., 2021).

To translate a 3D point selected on the mesh into 2D, ASTTRO uses the camera model provided in each image label to the position (in image pixel space) of a ray from the camera origin to the selected point. By computing this for each available image ASTTRO can determine the set of images that include the selected feature, and the



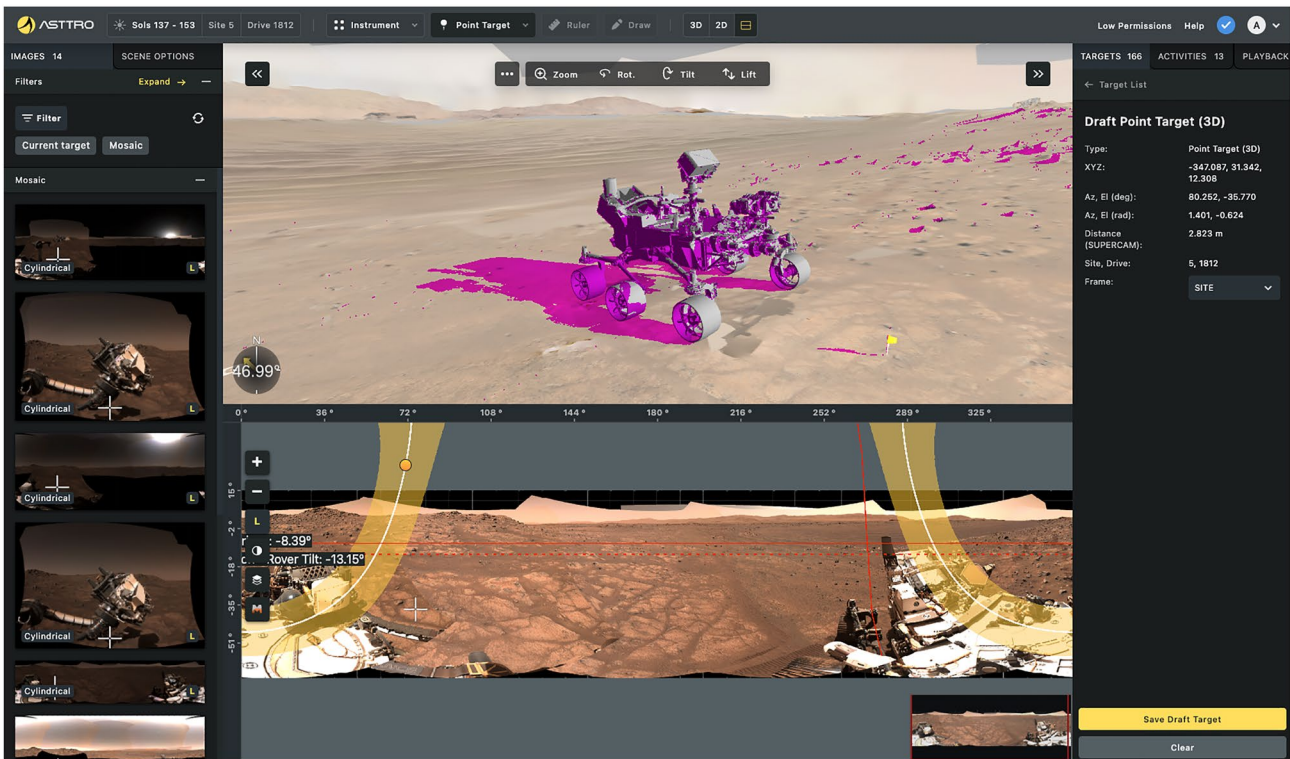


**Figure 11.** Top of the interface shows the contextual mesh product produced by Landform, which combines surface imagery with high resolution imaging science experiment imagery. The view shows shadows for a simulated time of day, and the sun path over 24 hr is displayed in the mosaic view in the bottom frame, to help with sun safety assessments.

position of the feature in each image. Conversely, ASTTRO can convert a 2D point selected in an image into 3D by either using the cartesian XYZ position provided in the accompanying XYZ RDR product, which is derived from stereo correlation, or by projecting a ray through the camera model and computing the intersection with the terrain mesh.

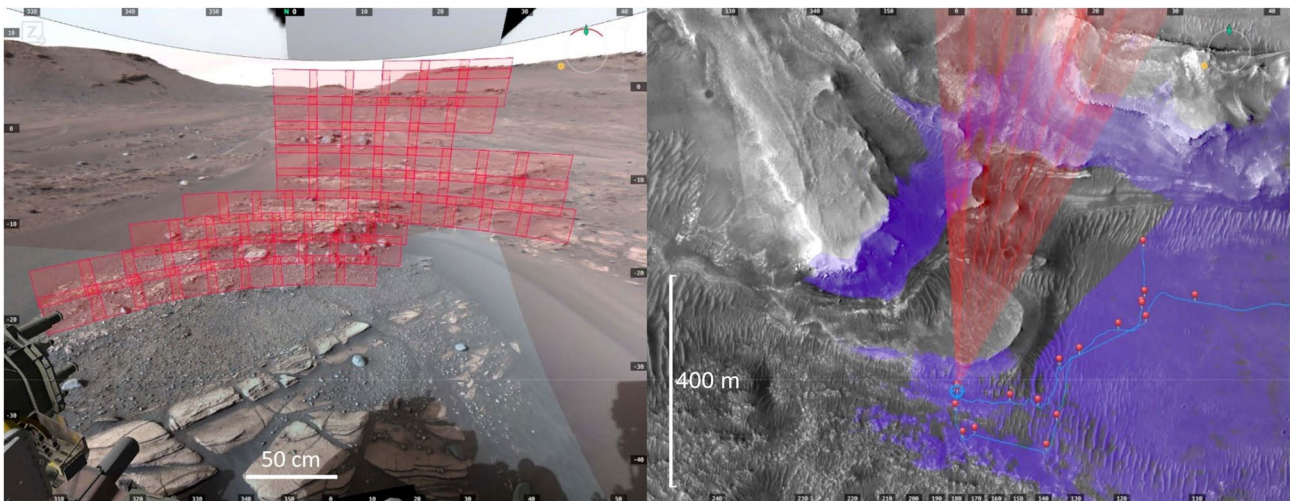


**Figure 12.** This is an option that was considered in Viewpoint for planning on Sol 423 for a Mastcam-Z 110 mm mosaic covering the Amaluk gray rock outcrop. The left screenshot shows the mosaic footprints from the camera's perspective on a scene of Navcam 2D images projected onto downsampled XYM meshes and the high resolution imaging science experiment (HiRISE) mesh. The right screenshot shows an overhead view of the same footprints on the HiRISE mesh. The purple region indicates the camera's viewshed at that rover location.

#### 5.4. Viewpoint 3D Visualization for Planning

Viewpoint is a 3D tool designed for planning imaging observations with cameras on rovers. It has two software adaptations that support Mars 2020 operations. One is a Mastcam-Z team tool used by the Mastcam-Z camera operators and team members. The other is specialized for the WATSON camera, used by the WATSON camera operators (see Text S6 in Supporting Information S1).

The Viewpoint client application models the rover state and camera perspectives in a simulated Martian environment constructed from Navcam, Hazcam, Mastcam-Z, and HiRISE data. Footprints (a visual representation of the camera field of view in the scene), can be laid out on the terrain to construct mosaics, which can then be translated into imaging commands. Additionally, Viewpoint provides the user with tools to assess Sun lighting and shadowing, rover mobility, targeting, time conversion, viewsheds, and object measurements.

##### 5.4.1. Viewpoint Data Sets

Viewpoint imports and displays four types of terrain mesh data products. It is currently using a HiRISE basemap imported from the publicly released USGS HiRISE orthomosaic and DTM of Jezero crater. The other three types of meshes are imported or derived from IDS produced data products. The following mesh products are supported.

1. HiRISE mesh.

The HiRISE mesh is useful for a few purposes such as planning imaging observations after a drive when no other meshes are available, assessing a camera's viewshed at future potential drive locations, and providing the means to point the cameras accurately in ground meshes taken from previous rover stopping locations. The rover accumulates error in its position knowledge as it drives, which can cause significant pointing uncertainty when the cameras are pointed at features in meshes acquired at previous stopping locations. Localizing the meshes acquired at each stopping location to the HiRISE basemap provides the relative translation offset between stopping locations which can be used to correct the error in the rover's position knowledge, so that camera operators can point the cameras accurately using meshes taken at previous rover locations. Customarily, the localized position of each rover stopping location is measured in a ground-based cartesian coordinate system ( $X$ : north,  $Y$ : east,  $Z$ : nadir) with the origin defined at the rover's landing site position. The rover's position in a global reference frame is rarely useful for tactical planning, so is not computed or provided to the user. The localization of a rover position can be performed in Viewpoint by dragging and dropping terrain meshes that were acquired at that location until features closely align with the features in the HiRISE basemap. Alternatively, localization may be performed by using tie points. Alignment along the nadir axis is done by a settling routine that minimizes the difference in distance along that axis between the meshes within user specified radius from the rover location. The source data for this mesh are available at (USGS, 2022).

2. IDS produced terrain meshes in OBJ format.

These meshes model surface features with densely spaced vertices. This is useful in cases where high fidelity surface shape is needed, such as when modeling terrain surface self-shadowing. However, it can be taxing on client computers to display many of these at once because of the large number of vertices.

3. Meshes made from downsampled IDS XYM products.

These are created by the Viewpoint server using the data in the XYM products (rover masked xyz coordinates in site frame). They model surface features more coarsely with a lower vertex density than the IDS produced OBJ meshes, which is often sufficient to accurately point cameras mounted to a mast assembly. Since they have less vertices, a user can load more of them at once before noticeably affecting the performance on the client computer. To help reduce clutter in the scene when many meshes are loaded from various rover locations, a resolution quality index is assigned to each vertex, so the user can use a slider to cull the rendering of mesh triangles that are below a threshold resolution.

4. Meshes made from 2D images (IDS RAD products).

Meshes that display 2D images are dynamically generated by the client at runtime by raycasting a grid of vectors derived from the camera models (provided in the PDS image header), to create a mesh that conforms to previously loaded mesh surfaces in the scene. These are useful when pointing the cameras at objects that are not present in other meshes, such as far away objects and the horizon. They can also provide higher resolution textures on lower resolution meshes. For instance, a high resolution Mastcam-Z 2D image can be projected onto a lower resolution Navcam mesh. While there can be a small amount of error in coregistration between image products from different cameras, this is generally insignificant when compared to the field of view of a Mastcam-Z footprint, so doesn't contribute much uncertainty to the pointing modeling.



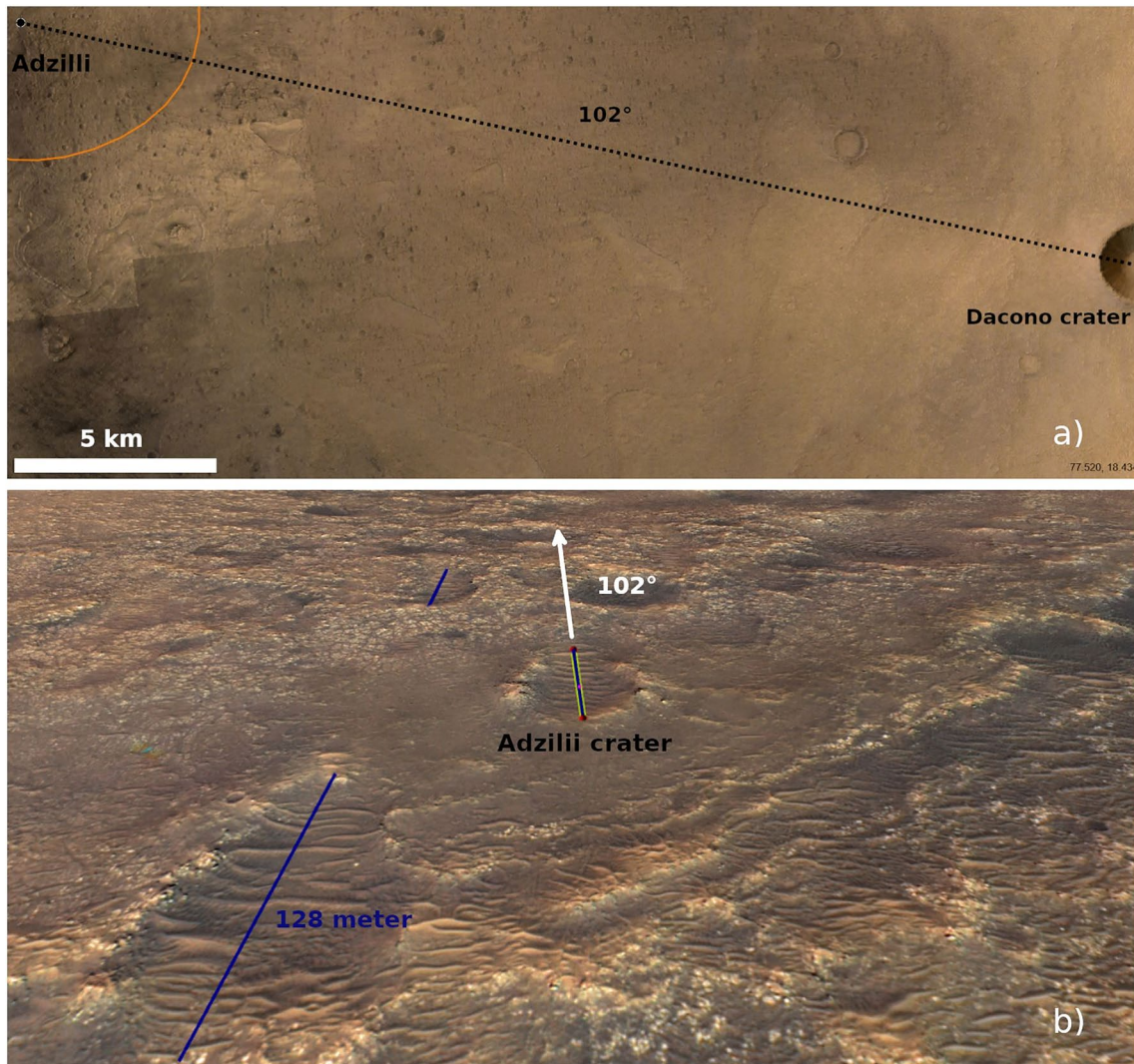


**Figure 13.** (a) Potential flight trajectory from Dacono crater to Adzilli crater with an orientation of  $102^\circ$  from north. Dacono crater is a fresh primary impact crater with a diameter of 2 km located in Jezero Crater. (b) Adzilli crater and the neighboring impact craters of the secondary crater cluster. The measurement of the elongated axis of Adzilli with PRo3D on a high resolution imaging science experiment Ordered Point Cloud revealed the same orientation as the potential flight trajectory from Dacono shown in (a).

Further information about the Viewpoint deployment structure and rendering modes can be found in Text S7 in Supporting Information S1.

#### 5.4.2. Display Within Viewpoint

Similar to the method that 2D images are displayed, footprint meshes are dynamically generated by raycasting from camera model vectors. The camera models are obtained by using kinematic models of the mast assembly to transform the calibration camera models according to the mast joint angles. Footprint meshes are created by raycasting along vectors derived from the camera model at the center and boundary of the subframe (the subset of the sensors on the detector that will be used for acquiring the image). See Figure 12 for examples.

In addition to their primary purpose of displaying the estimated scene content of an image command, the footprint vertex coordinates are used for other purposes, including footprint overlap latching, coordinate frame conversions, focus setting algorithms, and detection of rover hardware imaging. Additionally, the center coordinates can be used to determine the mast slew angles necessary to center one camera over the field of view of the other, which is useful in cases like multispectral imaging when it is desired to maximize overlap between the left and right cameras (Figure S22 in Supporting Information S1).

## 6. Mastcam-Z 3D Vision Data Products and Presentation Science Use Cases

This section contains a representative set of science use cases for 3D exploitation of Mastcam-Z data. It is not meant as a 1:1 instruction set how to proceed or reproduce the results, but to explain in a summarized way the context to relevant science applications, whilst allowing the reader to reproduce the results, as these parts are emphasizing the open source parts of the toolset.

### 6.1. Impact Science

Plate tectonics on Mars was not as active and long lasting as on the Earth (Golombek & Phillips, 2010). As a result, many more traces of meteoritic impacts accumulated on its planetary surface compared to the surface of the Earth. For example, the Mars 2020 mission landed within Jezero crater (Stack et al., 2020), an impact structure with a diameter of about 45 km that is most likely more than 2.6 Ga old (Shahrazad et al., 2019). Also, previous rover missions landed in impact craters (Wray, 2013) or impact structures, and even found some meteorites (Schröder et al., 2008) during their traverses on the surface of Mars. One of the open questions is, how to recognize rocks that, at least on Earth, would provide unambiguous evidence for impact cratering. As noted by French and Koeberl (2010), the only unambiguous macroscopic evidence for impact on Earth are shatter cones (all other evidence requires microscopic studies or geochemistry). Thus it was intriguing that Newsom et al. (2015) noted the presence of possible shatter cones in Curiosity Mars rover images, but these images were not convincing, possibly due to limited resolution. Our efforts include, therefore, the search for shatter cones in Perseverance images (cf., e.g., Koeberl et al., 2019, 2021). Also, wind-abrasion features (ventifacts) can have appearances similar to shatter cones, causing potential confusion (see, e.g., Figure 8 in French & Koeberl, 2010).

After its landing in the Jezero crater the traverse of Mars 2020 rover Perseverance headed to the south where it passed by a small secondary impact crater cluster. One crater of this secondary crater cluster named Adziilii crater was visited by Perseverance between Sols 104 and 110 (Calef, Almark, et al., 2021). Using a HiRISE OPC and PRo3D, the orientation of the elongated axis of the crater was measured and with this information the potential primary crater determined. In the case of a secondary crater like Adziilii the orientation of the elongated axis is the direction from where the ejecta block came from that formed the secondary crater (see Robbins & Hynek, 2014 and references therein). As can be seen from Figure 13, the orientation of the major axis of Adziilii crater (102° azimuth) is the same as the orientation of the potential flight trajectory from a sharp-rimmed, fresh-looking impact crater, that has a diameter of 2 km and lies approximately 28 km to the east, still within Jezero crater.

### 6.2. Analysis of Ventifacts

Some of the rocks near the Butler landing site appear to have been deeply abraded by wind-blown sand, forming features called ventifacts (Laitly & Bridges, 2008). Such features can easily be mistaken for shatter cones (and thus for evidence of impact processes). The orientation of linear features such as flutes on such ventifact-affected rocks records the direction of the strong winds that formed them. Candidate ventifacts were identified in Mastcam-Z mosaics with sufficiently high resolution to determine whether formation by wind abrasion is likely. Once ventifacts were confidently identified (based on experience gained on previous rover missions), the orientation of flutes and other linear features were measured using OPCs generated using Mastcam-Z stereo mosaics. For the analysis of ventifacts, PRo3D offers quantitative & true scale 1D, 2D and 3D annotation and statistical analyses of annotations (length, direction, altitude, elevation delta, orientation of planes, true thickness, dip and strike, areas, slopes, and other geometric relationships as directly to be obtained from the high-resolution OPC). Example measurements, acquired by selecting the ends of the aeolian abrasion features with the linear polyline tool, are shown in Figure 14.

Twenty Mastcam-Z stereo mosaics acquired by Sol 400 each included up to 21 features that were judged to be formed by eolian abrasion. The orientations of these features were measured as shown above and averaged for each mosaic. The average orientation of the data from the 20 mosaics is  $95 \pm 6^\circ$  measure clockwise from north. This is nearly the opposite direction relative to the orientation of wind tails and other indicators of recent winds, suggesting that the ventifacts were formed by strong winds in a different climate regime (Herkenhoff et al., 2023).

### 6.3. 3D Soil Crust Analysis

Understanding the physics and chemistry of the Martian soil is critical for future human exploration, as well as understanding samples that will be returned (Beatty et al., 2019). Previous work on Mars has identified evidence



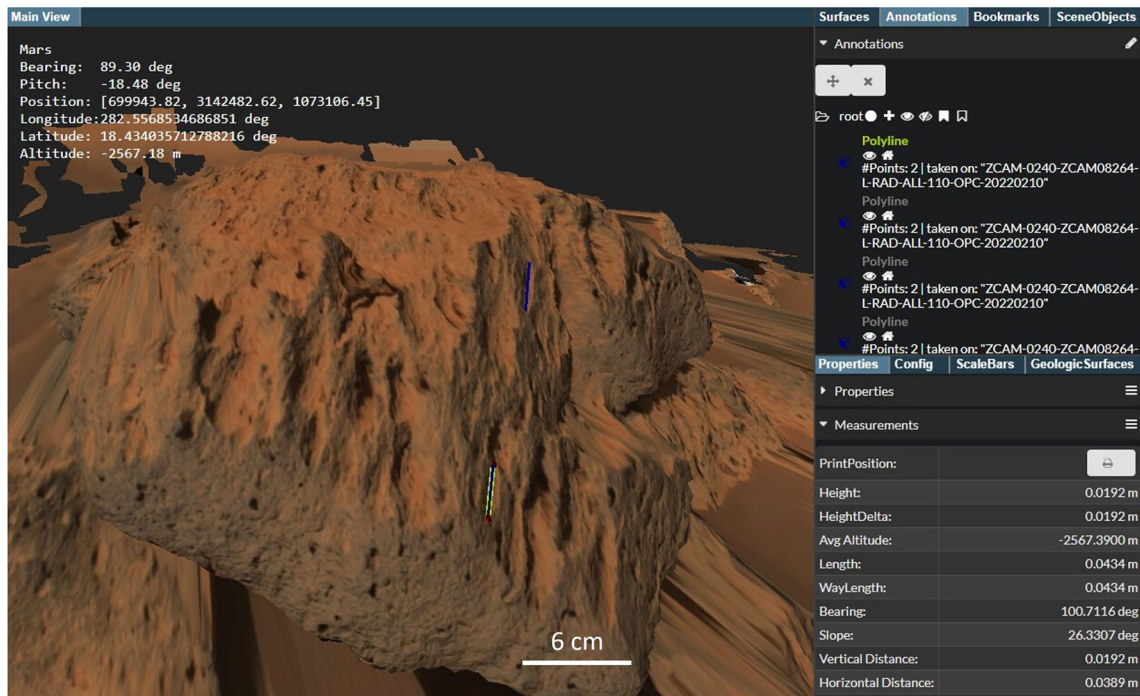


**Figure 14.** Screenshot of PRo3D display of Ordered Point Cloud generated using Mastcam-Z data acquired on Sol 240, showing measurements of two linear features on a ventifact.

of fractures in the soil surface that indicate the presence of crust in multiple locations site (e.g., Blake et al., 2013; Sullivan et al., 2008) indicating that this is a common phenomenon on Mars. The characteristics of the crust and extent of induration, as evidenced in the 3D observation of cracks and fractures, as well as tracks, sheds important light on the characteristics of the crust (Hausrath et al., 2023). The fractures indicate evidence of induration, which may also indicate the presence of hydration and salts.

The depth of the tracks (ranging from zero on solid surface to decimeter range in regolith), which can also be examined using 3-D imaging, also provides information about the compaction of the soils. On Earth, the compaction of the soil can be measured using a penetrometer, which yields the pressure of the penetration resistance. This penetration resistance has been linked to parameters such as the characteristics of the wheel tracks (Davidson, 1965). Measuring the depth of the wheel tracks using 3-D imaging therefore allows a comparison of such information for soils on Mars, starting with sub-mm depth evaluation at close-range, with range resolution degrading quadratically with distance.

An example of a measurement of the depth of rover tracks in PRo3D is shown in Figure 15a. Regions of the Martian soil that have a soil crust are indicated by rover tracks as shown in Figure 15b. From such stereo pair images, the corresponding OPC files for the measurements in PRo3D can be processed. The capability of such depth measurements using the OPCs depends on the viewing direction of the rover camera onto the rover tracks. The viewing direction must be more or less parallel to the rills of the rover tracks. A perpendicular viewing direction makes a meaningful measurement impossible because in this case the bottom of the rill is hidden and a 3D reconstruction of this part of the rover tracks from 2D images is therefore not possible. A further limitation is the range of the camera to the rover track. For stereo images of rover tracks taken at a distance of several meters, the resolution of the resulting OPCs is not good enough to allow meaningful measurements. The limit is given by the grid size of the 3D mesh on which the 3D reconstruction is based. The limit of the camera distance for measuring a 1 mm thin crust is around 2–3 m (ZCAM 110 mm).

#### 6.4. The Benefit of 3D Data Representations for Geology

In geology, an important part of the fieldwork is the assessment of spatial relationships between objects of geological interest. For remote sensing missions such as the Mars rover missions the capabilities of exploring the

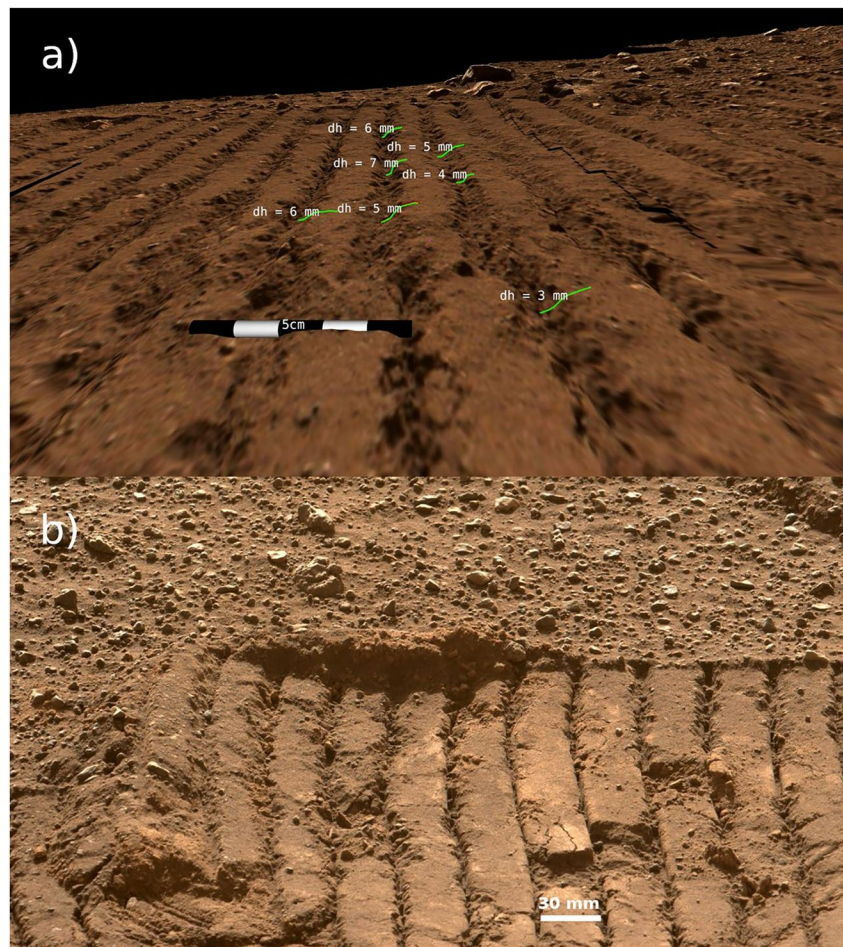


**Figure 15.** (a) This is an Ordered Point Cloud gained from a Mastcam-Z stereo sequence (Sol 46, sequence id ZCAM08011) by PRoViP shown in PRo3D with measurements of the depth of rover tracks. The morphological parameters of the rover tracks allow some conclusions to be drawn on the soil crust present in this area. (b) Example of a rover track as captured by Mastcam-Z on Sol 46 (sequence id ZCAM08011), showing a compacted regolith indicating the presence of a soil crust.

local outcrops are very limited and interpretation of spatial relationships are restricted to a few (stereo) images. However, due to proper planning, the most important phenomena are densely covered by stereo images and hence are processed to OPCs which can be further investigated fully virtually within 3D data analysis and interpretation assets like PRo3D.

Planar geologic features, such as bedding planes and faults, are quantified by a dip angle and strike azimuth which is perpendicular to the direction of the dip. Planar features in 3D models can be measured using either by solving the three point problem or by performing a regression on a 3D trace line that densely samples the surface and enables regression uncertainties to be assessed. Regressions on trace lines are preferable particularly for centimeter to meter scale outcrops that are largely linear to increase the statistical power of the measurements. A trace line for a strike dip measurement must adequately represent the geometry on orthogonal axes to constrain the planar fit. Lewis et al. (2008) developed a number of empirical mathematical criteria for determining if a planar fit was adequately constrained using Principal Components Analysis (PCA) on the trace line's coordinates by inspecting the ratio between the second and third components to ensure the fit is performed on data significantly larger than the out-of-plane error. PRo3D implements the PCA based regression methodology from Quinn & Ehlmann, 2019, which is best adapted to analysis of data with non vertical errors and represents the error space in spherical coordinates. As a final check, measured planes can be projected-out and visualized in PRo3D to assess the geologic reasonability of the orientation measurement in context with the surrounding outcrop to reduce errors from improper bedding surface interpretation. Examples of causes of improper mapping include rotations, faulting, deformation, diagenesis, or weathering of surfaces that corrupt the primary bedding surface (Stein



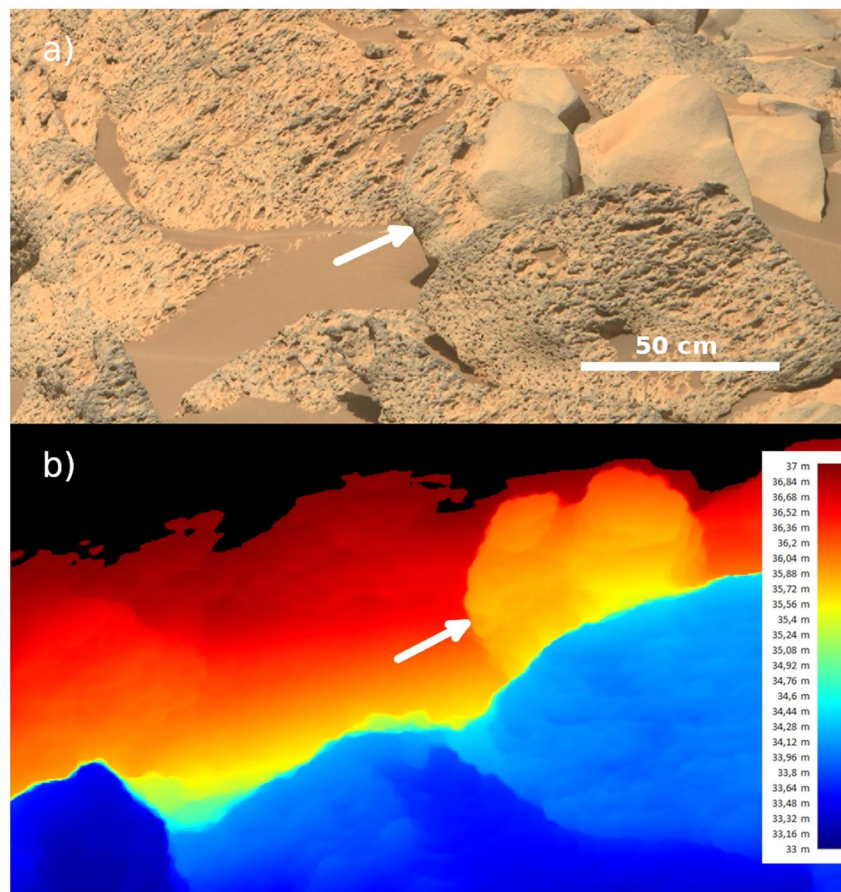


**Figure 16.** (a) Part of a Mastcam-Z image from Sol 112 (sequence id ZCAM08088) showing rocks in the vicinity of Adziilli crater. The rock marked with the white arrow shows two different surface expressions leading to the interpretation that this might be two different rocks. (b) The distance map shown here is a 2½D product derived from the Mastcam-Z stereo image pairs and shows that it is in fact one and the same rock.

et al., 2020). Improper mapping is a common source of error best mitigated by mapping the traces iteratively in a 3D visualization environment to permit real time corrections.

Uncertainties can lead to controversial interpretations. Due to the high power of statistical data (i.e., multiple supporting points in close range with 3D mm accuracy), human annotation or preliminary interpretation is still the largest source of errors.

An example is shown in Figure 16a. This is an image taken by NASA's Mars 2020 Rover Perseverance on Sol 112 in Jezero crater. At this point in the mission, the lithological diversity and the origin of the local rocks was the subject of extensive discussions. It was therefore interesting to know if the pitted surface and the massive surface are part of the same rock (marked with a white arrow), or if they represent two different rocks that are located very close one after the other. A distance map (see Figure 16b) from the corresponding Mastcam-Z stereo image pair showed that these two different surface textures must be part of one and the same rock.

Dip and strike measurements are imperative in gaining a quantitative understanding of the architectural geometries of rock bodies imaged by Mastcam-Z. Architectural observations can be combined with textural and geochemical observations to aid hypothesis testing for the science team. A typical workflow inspired by terrestrial field geology techniques can be applied to OPCs processed from Mastcam-Z stereo-mosaics in PRoViP within PRo3D, to place the dip and strike measurements in geological context for characterizing outcrop architecture. This workflow has been applied to OPCs reconstructed from image data collected on Sols 168 and 169 at the Mure outcrop (Figure 17), omitting the sedimentological aspects in order to present an example of a more general outcrop interpretation.

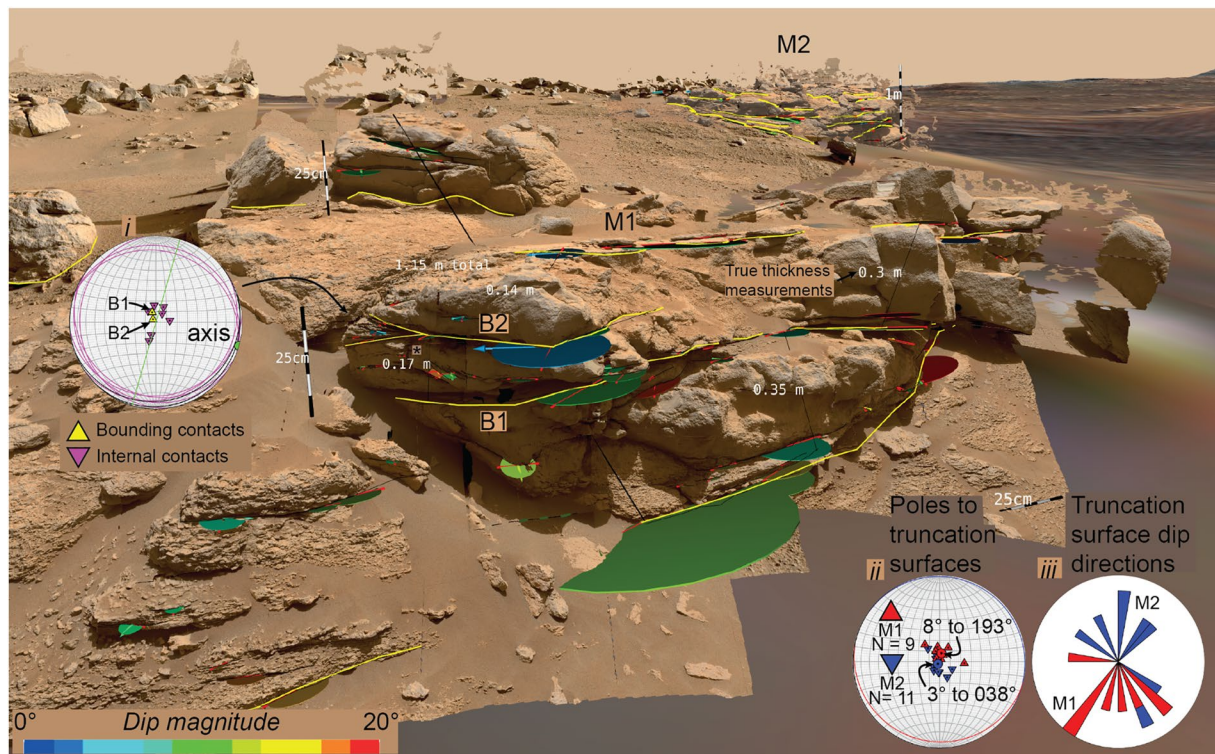


**Figure 17.** Interpretation of the Mure outcrop, at the boundary between the Seitah and Máaz formations in Jezero crater, in PRo3D, based on Ordered Point Clouds processed from Mastcam-z stereo-mosaics collected on Sols 168–169 (Mastcam-Z sequence ids 8180–8182). Truncation surfaces which could be traced across the outcrop are shown as bold yellow lines. Dip and strike measurements are shown as disks, color coded by the dip magnitude recorded. Scale bars and true thickness measurements are labeled in PRo3D and the inset stereonet (i–iii) illustrate the geometrical analysis of key mapped layer contacts. 3D scale bars are inserted in different parts of the scene to illustrate local scale.

After initial adjustment of rendering preferences (priority rendering, brightness, contrast, resolution, geometry filtering), the initial stage of the virtual outcrop interpretation workflow involved inspection of the outcrop, measurement of key outcrop dimensions, collecting bookmarks of regions of interest and placing scale bars. This process allows the user to better visualize the outcrop geometries and understand the spatial distribution and basic dimensions. Key features to observe in such a visual inspection of the 3D data—in conjunction with the image mosaics—are rock layers in the outcrop, changes in texture and relative color, abrupt changes in topographic slopes, identification of contacts which can be traced and correlated and any internal structures present.

The second stage of the workflow involved tracing key layer contacts across the outcrop, and mapping of truncated contacts, wherein a layer contact abuts against another contact. Basal contacts between apparently different rock types and primary layering or bedding are important features in determining regional dip and strike patterns with respect to small scale local deviations due to internal structures and any deformation if present. At Mure (Figure 17), the basal surface contacts and truncation surface contacts (yellow lines in Figure 17) were mapped on two outcrops (M1 and M2), which protrude from the surrounding knobby bedrock, and show a relatively smooth texture in outcrop, as well as internal contacts which can be traced up to ~1.5 m across. Different line symbologies (based on color and weight) can be used to interpret different hierarchies of layer contacts or other physical features present. At Mure, lobate internal geometries within the yellow bounding contacts were identified which consistently abutted the truncation surfaces (not shown in Figure 17).

The interpretations from stage 2 are used to guide collection of dip and strike measurements in the third stage of the workflow. The orientations of the truncation surfaces mapped are plotted in the inset stereonet and rose diagram (Marshak & Mitra, 1988) in Figure 17 (ii and iii). These data show a predominantly southwest dip in M1 averaging 8°–193° and a spread in dip directions between the southeast and west. The truncation surface dips in M2 have an average dip of 3°–38°, and a larger spread between the northwest and southeast. The truncation surface dips were used to measure the true thickness of the M1 outcrop and its internal elements (white text in



Figure 17). The cumulative maximum thickness of M1 is 1.15 m, and internal elements are 0.15–0.35 m thick. The fourth stage of interpretation involves collecting the orientations of internal features, which are represented by the smaller dip and strike disks in Figure 17. These vary significantly with respect to the basal surfaces, dipping in multiple directions and generally steeper dips than the underlying truncation surface, possibly reflecting lobate layer geometries. The inset stereonet (*i*) in Figure 17 shows an analysis of the antiformal structure marked with an asterisk, between truncation surfaces B1 and B2. The B1 surface dips 10°–161°, and the B2 surface has a sub-parallel dip of 4°–139°. Between these surfaces the antiformal feature has a southern limb which dips approximately 12°–195° and a northern limb which dips approximately 15°–018°. A  $\pi$ -girdle analysis of this structure shows that it has a horizontal axis trending to 106°, sub-parallel to the underlying surface strike.

## 7. Conclusions and Outlook

The Mars 2020 Mastcam-Z investigation provides a comprehensive 3D vision and visualization database that has shown to be essential for the interpretation of Mars 2020 planetary science context. The assets for processing and visualization available within the mission and for further public data exploitation are summarized, and relevant scientific use cases of 3D vision and visualization are demonstrated. The paper provides a first attempt to describe all primary 3D vision assets (data, processing and visualization) for mission-relevant tactical and strategic down- and uplink within the Mars 2020 mission in the context of science return.

Mastcam-Z 3D vision and visualization is an excellent example of collaborative exploitation of space exploration mission data, despite the involvement of international partners with heterogeneous background, tools and objectives. 3D data assets are a complex field with many degrees of freedom, yet data and results' exchange within the mission still works smoothly, efficient and without any friction. Nevertheless, the understanding of the entire team about the individual strength and peculiarities and shortcomings of the individual tools and product classes is still growing, and further thoughts about self-critical analysis of currently existed methodologies and approach of the solutions to present state-of-art, in particular in the field of stereo image processing, calibration and SfM are subject to future work. In addition, there is still some potential for improvement and opening of new opportunities for science gain, to name a few, just from the open-access inspired PRo3D domain.

- Storytelling is one of the best methods to efficiently explain how a geologic interpretation was carried out. It allows to guide peers, students and the interested public through important steps of the process. In this way it supports collaboration and dissemination. VRVis is already investigating storytelling mechanisms that are directly embedded into PRo3D. In a prototype scientists can create a storyboard while carrying out an interpretation. Afterward a video can be created from it and augmented with a narration. VRVis will enhance storytelling for PRo3D in the future, especially coupling it with provenance tracking and increasing its usability.
- Provenance tracking is a further research topic concerning PRo3D. It stores how products were created or obtained, by whom and when. This makes the whole workflow of a scientific investigation reproducible and comprehensible and thus supports multi-disciplinary collaboration. It includes all steps such as raw data capturing, processing and interpretations by planetary scientists (derived products). Provenance information increases the reliability of products as their origin becomes clear and also the uncertainties associated with this process. VRVis is currently researching provenance tracking and visualization. A prototype visualizes provenance as a graph that is interactive to query information for each single step of an analysis workflow. In combination with storytelling, it also becomes a powerful tool to revisit and mediate the whole workflow of a rover mission campaign.
- The View Planner of PRo3D is currently extended to find optimal long baseline stereo positions. For that use case it is important to simultaneously visualize instrument footprints from different rover locations so that overlapping regions can be identified. Also, the simulated view of instruments should allow a direct visual comparison of two positions. Additionally, we want to calculate view sheds from waypoints of a rover traverse. This is a rather coarse estimation of what is visible from the rover's mast and does not consider particular instruments or their settings. Nevertheless, view sheds allow identifying serendipitous spots for long baseline stereo images both along the previous and the planned rover paths. They will be shown as a colored region on the DTM.
- Collaboration in combination with real-time (local) access to highest fidelity and resolution data is another important topic of future research.

## Abbreviations and Acronyms

2D	Two-dimensional
3D	Three-dimensional
3DTiles	Specification for streaming massive heterogeneous 3D geospatial data sets
AMMOS	Advanced Multi-Mission Operations System
ARM	Arm Reachability data product
ASTTRO	Advanced Science Targeting Toolkit for Robotic Operations
ASU	Arizona State University
AWS	Amazon Web Services
BOTH	Fixed stereo arrangement (two cameras as mounted on joint rig)
BRDF	Bidirectional Reflectance Distribution Function
CalTech	California Institute of Technology
CAMP	Campaign Analysis Mapping and Planning tool
CCD	Charge-coupled device
COTS	Commercial-off-the-shelf
CSV	Comma-separated values
DN	Digital number
DSP	Stereo correlation data product ("Disparity")
DTM	Digital terrain model
EBY	De-Bayered image product
ECM	Telemetry processing
EDR	Experiment data record
EFS	Elastic File System
EPO	Education, Publication and Outreach
ESA	European Space Agency
FDR	Fundamental Data Record
FOSS4G	Free and Open Source Software for Geospatial
FoV	Field-of-View
GeoJSON	Geospatial JavaScript Object Notation
GIS	Geographical Information System
GUC	Arm Goodness data product (acronym)
GUH	Helicopter Goodness data product (acronym)
GUI	Graphical User Interface
HIRISE	high resolution imaging science experiment
IAU	International Astronomical Union
IDS	Instrument Data System
InSight	Interior Exploration using Seismic Investigations, Geodesy and Heat Transport (NASA Mars Lander 2018)
IR	Infrared
JPL	Jet Propulsion Laboratory
JR	JOANNEUM RESEARCH
kd-Tree	k-dimensional Tree: Data structure to support a 3D data representation
LBS	Long-Baseline-Stereo
LoD	Levels-of-Detail
M2020	Mars 2020
MER	Mars Exploration Rover
MIPL	Multimission Image Processing Laboratory
MMGIS	NASA AMMOS GIS
MOLA	Mars Orbiter Laser Altimeter
MSL	Mars Science Laboratory
MSSS	Malin Space Science Systems
NASA	(United States) National Aeronautics and Space Administration
ND	Neutral Density
OBJ	geometry definition file format (acronym)

OPC	Ordered Point Cloud
PCA	Principal Components Analysis
PDS	Planetary Data System
PI	Principal Investigator
PRo3D	Planetary Robotics 3D Viewer
PRoViP	Planetary Robotics Vision Processing
RAD	Radiometrically corrected image product
RAS	Radiometrically corrected image product
RDR	Reduced Data Records
RGB	Red Green Blue
RMI	Remote Micro-Imager
RNG	Range data product
RSM	Remote Sensing Mast
RSVP	Robot Sequencing and Visualization Program
RUF	Roughness data product (acronym)
S3	Simple Storage Service
SfM	Structure-from-Motion
SLP	Slope data product
Sol	One sol is a Martian Day = 24 hr, 37 min and 22 s
TFH	Helicopter Placement data product (acronym)
TMS	Tile Map Service
USGS	United States Geological Survey
UVW	Surface Normal data product (acronym)
VICAR	Video Information Communication and Retrieval
VIPER	NASA's Volatiles Investigating Polar Exploration Rover
WATSON	Wide Angle Topographic Sensor for Operations and eEngineering
WebGL	Web Graphics Library
XYZ	XYZ data product
ZCAM	Mastcam-Z

#### Acknowledgments

The authors would like to thank the reviewers for their time and efforts and sincerely appreciate the valuable comments and advice to improve the manuscript in the spirit of its objectives. JOANNEUM RESEARCH, VRVis and the Austrian Academy of Sciences receive/d funding from ESA PRODEX Contract PEA 4000117520 and from the Austrian Research Promotion Agency, ASAP-18 Project 892662 “Mars-3D”. VRVis is funded by the Austrian Ministry of Climate Action and Energy, the Austrian Federal Ministry for Digital and Economic Affairs, Styria, the Styrian Business Promotion Agency, Tyrol, and the Vienna Business Agency in the scope of COMET—Competence Centers for Excellent Technologies (879730) which is managed by the Austrian Research Promotion Agency. Opocode LLC receives funding from Arizona State University for development of Viewpoint for Mastcam-Z, and from Malin Space Science Systems for development of Viewpoint for WATSON. S. Gupta receives UKSA funding (ST/X002373/1). A portion of this research was carried out at the Jet Propulsion Laboratory, California Institute of Technology, under a contract with the National Aeronautics and Space Administration (80NM0018D0004). Funding for the U.S.-based authors of this work was provided by the National Aeronautics and Space Administration's Mars 2020 Project, either directly or via subcontracts from the California Institute of Technology's Jet Propulsion Laboratory and Arizona State University (subcontract 1411125).

#### Data Availability Statement

Mars 2020 Mastcam-Z source images are available on <https://mars.nasa.gov/mars2020/multimedia/raw-images/> (Mastcam-Z, 2022). Their PDS-released counterparts, including IDS-processed results, are available on [https://pds-geosciences.wustl.edu/missions/mars2020/mars2020\\_dois.htm](https://pds-geosciences.wustl.edu/missions/mars2020/mars2020_dois.htm) under the table entry “Mast Camera Zoom Bundle” (Bell & Maki, 2022). Ordered Point Clouds (OPCs) as processed by PRoViP from all PDS-released Mastcam-Z stereo and monoscopic data sets are available from `sftp://PRoViP-Mastcam-Z-PDS-Released@dig-sftp.joanneum.at:2200`—with user `PRoViP-Mastcam-Z-PDS-Released` and password `MQRr63hJdUzVFHYc!`. The one-click access link is `sftp://PRoViP-Mastcam-Z-PDS-Released:MQRr63hJdUzVFHYc!@dig-sftp.joanneum.at:2200/AnOPCfromHiRISEDTM/Ortho(monochrome)` is available on `sftp://PRoVi-OpenAccess@dig-sftp.joanneum.at/Mars/MARS-2020/HiRISE/OPC`—with user `PRoVi-OpenAccess` and password `LMWasdwd!201423!g`. The one-click access link is `sftp://PRoVi-OpenAccess:LMWasdwd!201423!g@dig-sftp.joanneum.at/Mars/MARS-2020/HiRISE/OPC/`. OPCs from MSL Mastcam stereo data are available from `dig-sftp.joanneum.at`—with user `MSL` and password `WH549!bjABu`. The one-click access link is `sftp://MSL:WH549!bjABu@dig-sftp.joanneum.at/`. Mastcam-Z Sketchfab models are available under the Mastcam-Z Sketchfab page: <https://sketchfab.com/Mastcam-Z>. Further sources for Mastcam-Z 3D data and data presentation are given in Text S8 in Supporting Information S1.

#### References

- Abarca, H., Deen, R., Hollins, G., Zamani, P., Maki, J., Tinio, A., et al. (2019). Image and data processing for InSight lander operations and science. *Space Science Reviews*, 215(2), 1–53. <https://doi.org/10.1007/s11214-019-0587-9>
- Abercrombie, S. P., Menzies, A., Abarca, H. E., Luo, V. X., Samochina, S., Trautman, M., et al. (2019). Multi-platform immersive visualization of planetary, asteroid, and terrestrial analog terrain. *Paper presented at 50th Lunar and Planetary Science Conference*.
- Balaram, J., Aung, M., & Golombek, M. P. (2021). The ingenuity helicopter on the perseverance rover. *Space Science Reviews*, 217(4), 56. <https://doi.org/10.1007/s11214-021-00815-w>



- Barnes, R., Gupta, S., Traxler, C., Ortner, T., Bauer, A., Hesina, G., et al. (2018). Geological analysis of Martian rover-derived digital outcrop models using the 3-D visualization tool, planetary robotics 3-D viewer—PRO3D. *Earth and Space Science*, 5(7), 285–307. <https://doi.org/10.1002/2018ea0003744>
- Beaty, D. W., Grady, M. M., McSween, H. Y., Sefton-Nash, E., Carrier, B. L., Altieri, F., et al. (2019). The potential science and engineering value of samples delivered to Earth by Mars sample return. *Meteoritics & Planetary Sciences*, 54, 667–671. <https://doi.org/10.1111/maps.13242>
- Bell, J. F., & Maki, J. N. (2022). Mars 2020 mast camera Zoom data Bundle [Dataset]. Planetary Data System. <https://doi.org/10.17189/1522843>
- Bell, J. F., Maki, J. N., Mehall, G. L., Ravine, M. A., Caplinger, M. A., Bailey, Z. J., et al. (2021). The Mars 2020 perseverance rover mast camera Zoom (Mastcam-Z) multispectral, stereoscopic imaging investigation. *Space Science Reviews*, 217(1), 1–40. <https://doi.org/10.1007/s11214-020-00755-x>
- Blake, D. F., Morris, R. V., Kocurek, G., Morrison, S. M., Downs, R. T., Bish, D., et al. (2013). Curiosity at Gale crater, Mars: Characterization and analysis of the Rocknest sand shadow. *Science*, 341(6153), 1239505. <https://doi.org/10.1126/science.1239505>
- Calef, F. J., Almark, S., Amudsen, H. E. F., Bechtold, A., Bell, J., Quentin, C., et al. (2021). Visiting a fresh crater in Jezero with the Mars 2020 Perseverance Rover. Paper (#14-10) presented at Geological Society of America Connects, Portland, Oregon. <https://doi.org/10.1130/abs/2021AM-370948>
- Calef, F. J., Soliman, T., Roberts, J., Chung, A., Abarca, H., & Dahl, L. (2021). NASA AMMOS multi-mission geographic information system (MMGIS) version 2.0: Updates and mission operations. Paper (#7061) presented at 5th Planetary Data and 2nd Planetary Science Informatics & Data Analytics Meeting.
- Coates, A. J., Jaumann, R., Griffiths, A. D., Leff, C. E., Schmitz, N., Josset, J. L., et al. (2017). The PanCam instrument for the ExoMars Rover. *Astrobiology*, 17(6–7), 511–541. <https://doi.org/10.1089/ast.2016.1548>
- Cozzi, P., Lilley, S., & Getz, G. (Eds.) (2019). 3D tiles specification 1.0. (Open Geospatial Consortium Standard 18-053r2). Retrieved from <http://www.opengis.net/docs/CS/3DTiles/1.0>
- Davidson, T. D. (1965). Penetrometer measurements. In C. A. Black (Ed.), *Methods of soil analysis. Part 1. Agronomy Monographs* (Vol. 9, pp. 472–484). <https://doi.org/10.2134/agronmonogr9.1.c37>
- Deen, R. G. (2003). Cost Savings through multimission code reuse for Mars image products. In *Proceedings of 5th International Symposium on Reducing the Cost of Spacecraft ground Systems and Operations, Pasadena, California*. Retrieved from <https://descanso.jpl.nasa.gov/RCSGSO/Paper/A0075Paper.pdf>
- Duxbury, E., & Jensen, D. (1994). *Vicar user's guide*. (Document D, 4186). National Aeronautics and space administration, Jet Propulsion Laboratory, The California Institute of Technology.
- Ferguson, R. L., Hare, T. M., Mayer, D. P., Galuszka, D. M., Redding, B. L., Smith, E. D., et al. (2020). Mars 2020 terrain relative navigation flight product generation: Digital terrain model and orthorectified image mosaics. Paper (#2020) presented at 51st Lunar and Planetary Science Conference.
- French, B. M., & Koeberl, C. (2010). The convincing identification of terrestrial meteorite impact structures: What works, what doesn't, and why. *Earth-Science Reviews*, 98(1–2), 123–170. <https://doi.org/10.1016/j.earscirev.2009.10.009>
- Fuhrmann, S., & Goesele, M. (2014). Floating scale surface reconstruction. *ACM Transactions on Graphics*, 33(4), 1–11. <https://doi.org/10.1145/2601097.2601163>
- Golombek, M. P., & Phillips, R. J. (2010). Mars tectonics. In T. R. Watters & R. A. Schultz (Eds.), *Planetary tectonics* (pp. 183–232).
- Hausrath, E., Adcock, C. T., Bechtold, A., Beck, P., Benison, K., Cardarelli, E. L., et al. (2023). An examination of soil crusts on the floor of Jezero Crater, Mars. *Journal of Geophysical Research: Planets*. in press. <https://doi.org/10.1029/2022JE007433>
- Hayes, A. G., Corlies, P., Tate, C., Barrington, M., Bell, J. F., Maki, J. N., et al. (2021). Pre-flight calibration of the Mars 2020 Rover Mastcam Zoom (Mastcam-Z) multispectral, stereoscopic imager. *Space Science Reviews*, 217(2), 29. <https://doi.org/10.1007/s11214-021-00795-x>
- Herkenhoff, K., Sullivan, R., Newman, C., Paar, G., Baker, M., Viudez-Moreiras, D., et al. (2023). Comparison of ventifact orientations and recent wind direction indicators near the Mars 2020 Octavia E. Butler landing site on Mars. JGR. in press.
- Kazhdan, M., Bolitho, M., & Hoppe, H. (2006). Poisson surface reconstruction. Paper presented at Eurographics Symposium on Geometry Processing, Cagliari, Italy.
- Kirk, R. L., Howington-Kraus, E., Rosiek, M. R., Anderson, J. A., Archinal, B. A., Becker, K. J., et al. (2008). Ultrahigh resolution topographic mapping of Mars with MRO HiRISE stereo images: Meter-scale slopes of candidate Phoenix landing sites. *Journal of Geophysical Research*, 113(E3), E00A24. <https://agupubs.onlinelibrary.wiley.com/doi/pdfdirect/10.1029/2007JE003000>
- Koeberl, C., Bechtold, A., Paar, G., Traxler, C., Garolla, F., & Sidla, O. (2021). Planetary scientific target detection via deep learning: A case study for finding shatter cones in Mars rover images. Paper (#1209) presented at 52nd Lunar and Planetary Science Conference.
- Koeberl, C., Paar, G., Barnes, R., Gupta, S., Traxler, C., & Ortner, T. (2019). Planetary analog study at the Danakil Depression, Ethiopia, to test the visualization software PRO3D for MastCam instrument on Mars-2020. Paper (#2226) presented at 50th Lunar and Planetary Science Conference.
- Laity, J. E., & Bridges, N. T. (2008). Ventifacts on Earth and Mars: Analytical, field, and laboratory studies supporting sand abrasion and windward feature development. *Geomorphology*, 105(3–4), 202–217. <https://doi.org/10.1016/j.geomorph.2008.09.014>
- Lewis, K. W., Aharonson, O., Grotzinger, J. P., Squyres, S. W., Bell, J. F., Crumpler, L. S., & Schmidt, M. E. (2008). Structure and stratigraphy of home plate from the spirit Mars exploration rover. *Journal of Geophysical Research*, 113(E12), E12S36. <https://doi.org/10.1029/2007JE003025>
- Maki, J. N., Gruel, D., McKinney, C., Ravine, M. A., Morales, M., Lee, D., et al. (2020). The Mars 2020 engineering cameras and microphone on the perseverance rover: A next-generation imaging system for Mars exploration. *Space Science Reviews*, 216, 137. <https://doi.org/10.1007/s11214-020-00765-9>
- Malvar, H. S., He, L., & Cutler, R. (2004). High-quality linear interpolation for demosaicing of Bayer-patterned color images. In *IEEE International Conference on acoustics, speech, and Signal Processing* (Vol. 3, p. 485). <https://doi.org/10.1109/ICASSP.2004.1326587>
- Marshak, S., & Mitra, G. (1988). *Basic methods of structural geology*. Prentice Hall.
- Marsviewer. (2022). PDS Marsviewer [Software]. Last visited 2022-11-04. <https://pds-imaging.jpl.nasa.gov/tools/marsviewer/>
- Mastcam-Z. (2022). Mars 2020 Mastcam-Z source images. [Dataset]. Retrieved from <https://mars.nasa.gov/mars2020/multimedia/raw-images/-selectScienceCameras-Mastcam-Z>. Last visited 2023-03-01.
- McEwen, A. S., Eliason, E. M., Bergstrom, J. W., Bridges, N. T., Hansen, C. J., Delamere, W. A., et al. (2007). Mars Reconnaissance Orbiter's high resolution imaging science experiment (HiRISE). *Journal of Geophysical Research*, 112(E5), E05S02. <https://doi.org/10.1029/2005JE002605>
- MMGIS. (2022). MMGIS Github code repository [Software]. Last visited 2022-11-04. Retrieved from <https://github.com/NASA-AMMOS/MMGIS>
- National Aeronautics and Space Administration. (2021). Mars 2020 mission instruments overview. Retrieved from <https://mars.nasa.gov/mars2020/spacecraft/instruments/>

- National Aeronautics and Space Administration. (2022). Explore with Perseverance. accessed 2022-06-01. Retrieved from <https://mars.nasa.gov/mars2020/surface-experience>
- Newsom, H. E., Mangold, N., Kah, L. C., Williams, J. M., Arvidson, R. E., Stein, N., et al. (2015). Gale crater and impact processes – Curiosity’s first 364 Sols on Mars. *Icarus*, 249, 108–128. <https://doi.org/10.1016/j.icarus.2014.10.013>
- Paar, G., Deen, R. G., Muller, J.-P., Silva, N., Iles, P., Shaukat, A., & Gao, Y. (2016). Vision and image processing. In Y. Gao (Ed.), *Contemporary planetary robotics: An approach toward autonomous Systems* (pp. 105–179). John Wiley & Sons.
- Paar, G., Ortner, T., Traxler, C., Barnes, R., Balme, M., Schröder, C., & Banham, S. G. (2022a). Preparing 3D vision & visualization for ExoMars. In *Proceedings of 16th Symposium on Advanced Space Technologies in Robotics and Automation (ASTRA 2022)*. ESA/ESTEC. Retrieved from <https://www.vrvis.at/publications/pdfs/PB-VRVis-2022-017.pdf>
- Paar, G., Traxler, C., Bechtold, A., Barnes, R., Hausrath, E., Gupta, S., & Calef, F. (2022b). Flyover videos from annotated 3D Martian environments within minutes: The PRo3D sequence bookmark facility. *Paper (#EPSC2022-40) presented at EPSC Conference, Granada, Spain*. <https://doi.org/10.5194/epsc2022-40>
- PRo3D (2022). Planetary robotics 3D viewer GitHub page [Software]. Last visited 2022-11-07. <https://github.com/pro3d-space/PRo3D>
- Quinn, D. P., & Ehlmann, B. L. (2019). A PCA-based framework for determining remotely sensed geological surface orientations and their statistical quality. *Earth and Space Science*, 6(8), 1378–1408. <https://doi.org/10.1029/2018ea000416>
- Robbins, S. J., & Hynek, B. M. (2014). The secondary crater population of Mars. *Earth and Planetary Science Letters*, 400, 66–76. <https://doi.org/10.1016/j.epsl.2014.05.005>
- Ruoff, N. A., Deen, R. G., & Pariser, O. (2022). *Mars 2020 (M2020) software interface specification, camera instrument data products*. (JPL Doc ID: D-99960, February 2022). Jet Propulsion Laboratory. Retrieved from [https://pds-imaging.jpl.nasa.gov/documentation/Mars2020\\_Camera\\_SIS.pdf](https://pds-imaging.jpl.nasa.gov/documentation/Mars2020_Camera_SIS.pdf)
- Schröder, C., Rodionov, D. S., McCoy, T. J., Jolliff, B. L., Gellert, R., Nittler, L. R., et al. (2008). Meteorites on Mars observed with the Mars exploration rovers. *Journal of Geophysical Research*, 113(E6), E06S22. <https://doi.org/10.1029/2007JE002990>
- Shahzad, S., Kinch, K. M., Goudge, T. A., Fassett, C. I., Needham, D. H., Quantin-Nataf, C., & Knudsen, C. P. (2019). Crater statistics on the dark-toned, mafic floor unit in Jezero Crater, Mars. *Geophysical Research Letters*, 46(5), 2408–2416. <https://doi.org/10.1029/2018gl081402>
- Smith, D. E., Zuber, M. T., Frey, H. V., Garvin, J. B., Head, J. W., Muhleman, D. O., et al. (2001). Mars Orbiter Laser Altimeter: Experiment summary after the first year of global mapping of Mars. *Journal of Geophysical Research*, 106(E10), 23689–23722. <https://doi.org/10.1029/2000je001364>
- SPICE (2022). The Spice Toolkit [Software]. Last visited 2022-11-04. <https://naif.jpl.nasa.gov/naif/toolkit.html>
- Stack, K. M., Williams, N. R., Calef, F., Sun, V. Z., Williford, K. H., Farley, K. A., et al. (2020). Photogeologic map of the perseverance rover field site in Jezero Crater constructed by the Mars 2020 science team. *Space Science Reviews*, 216(8), 127. <https://doi.org/10.1007/s11214-020-00739-x>
- Stein, N. T., Quinn, D. P., Grotzinger, J. P., Fedo, C., Ehlmann, B. L., Stack, K. M., et al. (2020). Regional structural orientation of the mount sharp Group revealed by in situ dip measurements and stratigraphic correlations on the Vera Rubin ridge. *Journal of Geophysical Research: Planets*, 125(5), e2019JE006298. <https://doi.org/10.1029/2019JE006298>
- Sullivan, R., Arvidson, R., Bell, J. F., III, Gellert, R., Golombek, M., Greeley, R., et al. (2008). Wind-driven particle mobility on Mars: Insights from Mars Exploration Rover observations at “el Dorado” and surroundings at Gusev crater. *Journal of Geophysical Research*, 113(E6), E06S07. <https://doi.org/10.1029/2008JE003101>
- Traxler, C., Ortner, T., Hesina, G., Barnes, R., Gupta, S., & Paar, G. (2017). The PRo3D View Planner – Interactive simulation of Mars rover camera views to optimise capturing parameters. *Geophysical Research Abstracts*, (Vol. 19, pp. EGU2017–18752). EGU General Assembly.
- Traxler, C., Ortner, T., Hesina, G., Barnes, R., Gupta, S., Paar, G., et al. (2022). The PRoViDE framework: Accurate 3D geological models for virtual exploration of the Martian surface from rover and orbital imagery. In A. Bistacchi, M. Massironi, & S. Viseur (Eds.), *3D digital geological models*. <https://doi.org/10.1002/9781119313922.ch3>
- USGS. (2022). Mars 2020 Jezero Crater Landing Site Controlled Orthomosaics [Dataset]. Last visited 2022-10-30. Retrieved from <https://astrogeology.usgs.gov/maps/mars-2020-jezero-crater-landing-site-controlled-orthomosaics>
- Wiens, R. C., Maurice, S., Robinson, S. H., Nelson, A. E., Cais, P., Bernardi, P., et al. (2021). The SuperCam instrument suite on the NASA Mars 2020 rover: Body unit and combined system tests. *Space Science Reviews*, 217(1), 4. <https://doi.org/10.1007/s11214-020-00777-5>
- Wray, J. J. (2013). Gale crater: The Mars science laboratory/curiosity rover landing site. *International Journal of Astrobiology*, 12(1), 25–38. <https://doi.org/10.1017/S1473550412000328>

## References From the Supporting Information

- Agisoft, L. L. C. (2022). Agisoft Metashape 1.8.4—Professional edition: Agisoft LLC software [Software]. <https://www.agisoft.com/downloads/installer/>
- Kazhdan, M., Surendran, D., & Hoppe, H. (2010). Distributed Gradient-domain processing of planar and spherical images. *ACM Transactions on Graphics*, 29(2), 1–11. <https://doi.org/10.1145/1731047.1731052>
- Łabędź, P., Skabek, K., Ozimek, P., & Nytko, M. (2021). Histogram adjustment of images for improving photogrammetric reconstruction. *Sensors*, 21(14), 4654. <https://doi.org/10.3390/s21144654>
- Luebke, D., Reddy, M., Cohen, J. D., Varshney, A., Watson, B., & Huebner, R. (2003). *Level of detail for 3D graphics*. Morgan Kaufmann Publishers.
- NASA. (2022). Retrieved from <https://mars.nasa.gov/mars2020/multimedia/raw-images/>
- Ortner, T., & Tobler, R. F. (2009). VILMA data structure design. Retrieved from [https://github.com/aardvark-platform/OpcViewer/blob/master/VilmaDataStructures\\_20101803.pdf](https://github.com/aardvark-platform/OpcViewer/blob/master/VilmaDataStructures_20101803.pdf)
- Ortner, T., Paar, G., Hesina, G., Tobler, R. F., & Nauschnegg, B. (2010). Towards true underground infrastructure surface documentation. In M. Schrenk, V. V. Popovich, & P. Zeile (Eds.), *Proceedings of the Real Corp 2010* (pp. 1–10).
- Ortner, T., Traxler, C., Piringer, H., Fritz, L., Schimkowitz, M., Paar, G., et al. (2019). Minerva: A 3D GIS and visual analysis framework. In *Proceedings of 15th Symposium on Advanced Space Technologies in Robotics and Automation (ASTRA 2019)*. ESA/ESTEC.
- Varadhan, G., & Manocha, D. (2002). Out-of-core rendering of massive geometric environments (pp. 69–76). *Paper presented at IEEE Visualization*. <https://doi.org/10.1109/VISUAL.2002.1183759>